DuSA: Fast and Accurate Dual-Stage Sparse Attention Mechanism Accelerating Both Training and Inference

Chong Wu*
Dept of Electrical Eng
City University of Hong Kong
chongwu2-c@my.cityu.edu.hk
imroxaswc@gmail.com

Jiawang Cao*
Opus AI Research
gavin.cao@opus.pro

Renjie Xu*
Dept of Electrical Eng
City University of Hong Kong
harryxu950510@gmail.com

Zhuoheng Ran
Dept of Electrical Eng
City University of Hong Kong
zhuoheran2-c@my.cityu.edu.hk

Maolin Che†
School of Mathematics and Statistics
Guizhou University
chncml@outlook.com

Wenbo Zhu
Opus AI Research
vito.zhu@opus.pro

Hong Yan
Dept of Electrical Eng
City University of Hong Kong
h.yan@cityu.edu.hk

Abstract

This paper proposes the Dual-Stage Sparse Attention (DuSA) mechanism for attention acceleration of transformers. In the first stage, DuSA performs intrablock sparse attention to aggregate local inductive biases. In the second stage, DuSA performs interblock sparse attention to obtain long-range dependencies. Both stages have low computational complexity and can be further accelerated by memory acceleration attention mechanisms directly, which makes DuSA faster than some extremely fast attention mechanisms. The dual-stage sparse attention design provides a lower error in approximating vanilla scaled-dot product attention than the basic single-stage sparse attention mechanisms and further advances the basic sparse attention mechanisms to match or even outperform vanilla scaled-dot product attention. Even in some plug and play situations, DuSA can still maintain low performance loss. DuSA can be used in both training and inference acceleration. DuSA achieves leading performance in different benchmarks: long range arena, image classification, semantic segmentation, object detection, text to video generation, and long context understanding, and accelerates models of different sizes.

1 Introduction

The vanilla scaled-dot product attention (VSA) mechanism [1] is a core technique in transformers due to its ability to capture and model long-range dependencies [2]. However, the softmax operation after the scaled-dot product becomes the main bottleneck that makes the computational complexity of VSA the square of the sequence length and significantly limits efficiency of VSA [3].

*Equal contribution
†Corresponding author

39th Conference on Neural Information Processing Systems (NeurIPS 2025).

To improve efficiency, various attention acceleration methods have been proposed. Among them, FlashAttention [4] is a milestone in attention acceleration that provides an exact method of attention acceleration by optimizing memory input/output (I/O) operations. Its successors [5, 6] further improve memory efficiency. In addition to these memory acceleration attention mechanisms, other methods focus on optimizing the computation bound by using the kernel trick to find a linear approximation [2, 3, 7–19] or utilizing the sparsity of attention matrices to perform local attention operations [18, 20–30]. These methods are usually called computation acceleration attention mechanisms. Memory acceleration attention mechanisms can usually provide an exact attention operation to replace the vanilla scaled-dot product attention mechanism directly. However, they are usually hardware-aware and their computational complexity is still quadratic with respect to the sequence length [18]. Computation acceleration attention mechanisms are usually faster than memory acceleration attention mechanisms, and some of them [18, 29, 30] can be further accelerated by memory acceleration attention mechanisms. However, most of them have inferior performance compared to VSA and cannot directly replace VSA without training or tuning.

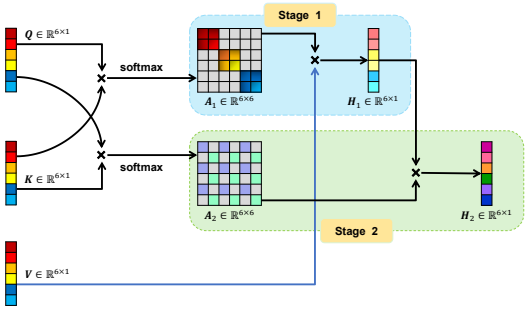

Figure 1: The overview of DuSA. Boxes with grey color denote zeros. Figs. 2 and 3 shows two examples for obtaining $\boldsymbol{A}_2$.

Figure 2: DuSA performs intrablock sparse attention within each block to obtain local inductive biases in Stage 1. DuSA performs interblock sparse attention to obtain global information in Stage 2. Here the blockify strategy is Strategy 1 in Remark 1. The different colors in attention matrices ($\boldsymbol{A}_1$ and $\boldsymbol{A}_2 = \boldsymbol{A}'$) denote the different blocks. The color changes between $\boldsymbol{V}$ and $\boldsymbol{H}_1$ and between $\boldsymbol{H}_1$ and $\boldsymbol{H}_2$ denote the information aggregation process.

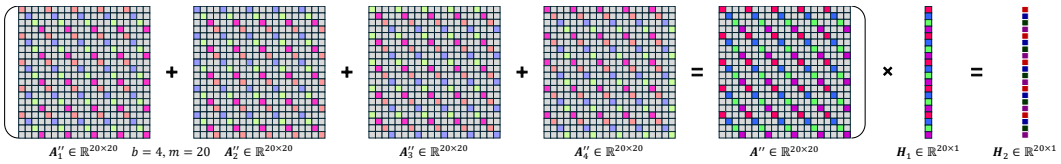

Figure 3: DuSA using Strategy 2 in interblock sparse attention can aggregate more information. $\boldsymbol{A}_2 = \boldsymbol{A}''$. $\boldsymbol{A}''_1 = \boldsymbol{A}'$ and $\boldsymbol{A}''_k$ $(k \neq 1)$ can be obtained using the rolling indices introduced in Remark 2.

This paper proposes Dual-Stage Sparse Attention (DuSA), a novel attention mechanism, for attention acceleration of transformers. This work builds on the basic single-stage sparse attention mechanisms [25] and advances the field further through the novel accurate dual-stage sparse attention mechanism design as shown in Fig. 1. DuSA performs intrablock sparse attention in the first stage and interblock sparse attention in the second stage, which makes DuSA capable of obtaining intrablock information (local inductive biases) and interblock information (long-range dependencies) at the same time and is significantly different from commonly used sparse attention mechanisms [23–25, 27–30]. Both

stages have low computational complexity and can be further accelerated by memory acceleration attention mechanisms directly. In summary, this paper has the following contributions.

(i) A novel and effective dual-stage sparse attention (DuSA) mechanism is proposed to significantly accelerate training and inference processes.

(ii) A mathematical relationship between DuSA and VSA is given: 1. The theoretical upper bound using DuSA to approximate VSA is derived. 2. The numerical results demonstrate that the dual-stage design has a lower approximation error than the single-stage design, despite the higher theoretical upper bound.

(iii) DuSA can approximate VSA with a low error: DuSA can maintain 97%+ performance using 75%-94% sparsity ratios by replacing VSA in vision transformers (ViTs) directly without training, and surpasses VSA after training.

(iv) DuSA surpasses state-of-the-art methods in terms of better performance and faster speed in different tasks.

2 Related work

Efficient attention mechanisms have been extensively studied to mitigate the quadratic complexity of attention. These methods can be classified into two categories based on their optimization focus: (1) memory acceleration methods and (2) computation acceleration methods.

2.1 Memory acceleration methods

Memory acceleration methods are usually hardware-aware and focus on minimizing memory I/O access to reduce complexity for some certain types of GPU architectures. FlashAttention [4] is the milestone for memory acceleration in attention computation. FlashAttention-2 (FA2) [5] is a major update version of FlashAttention, which further improves efficiency. FlashAttention-3 is a version that supports new features or characteristics of the new Hopper GPU architectures. Inspired by FlashAttention, some variants of FlashAttention have been proposed. FlashSigmoid [31] implements a memory efficient sigmoid attention mechanism based on FA2. Native sparse attention (NSA) [29] and SpargeAttn [30] implement memory efficient selective sparse attention based on FlashAttention. Different to NSA, SpargeAttn is designed only for inference acceleration, which cannot be used to accelerate the training process.

2.2 Computation acceleration methods

Computation acceleration methods can be classified into two types: (1) the linear kernelized attention mechanism; (2) the sparse/local attention mechanism according to whether or not the sparse property of the attention matrices is utilized.

2.2.1 Linear kernelized attention mechanisms

Linear kernelized attention mechanisms use the kernel trick to approximate the softmax normalization of the vanilla scaled-dot product of the query matrix and the key matrix into a linear product of two independent feature maps. Powerful feature map design becomes the key problem in this kind of efficient attention mechanism. Rectified linear unit (ReLU) [32] based feature maps are commonly used to approximate softmax normalization of the vanilla scaled-dot product of the query matrix and the key matrix, such as the ReLU-based feature map dividing by sequence length [9], the cubic ReLU-based feature map [7], the convolution-enhanced ReLU-based feature map [33], and the exponential linear unit (ELU) [34] based feature map [10]. In addition to ReLU-based feature maps, there are some other types of feature maps, such as the *cos*-based nonlinear feature map [14] and the independent softmax-based feature map [8, 15, 18]. The attention matrix is approximately low-rank [17], therefore, another kind of feature map design is based on low-rank decomposition methods, such as the Nyström approximation [2, 3, 12, 35], the CUR decomposition [17], the singular value decomposition (SVD) [36], and matrix decomposition [37].

2.2.2 Sparse/local attention mechanisms

Sparse/local attention mechanisms are based on the sparse property of attention matrices and usually use blockify methods, such as sliding windows, to partition the original sequences into smaller blocks [18]. Attention computation is limited within these blocks. Computational complexity can be reduced to almost sublinear complexity with an increasing number of blocks. Blockify methods based on sliding windows were first introduced by Longformer [24] and Swin [20]. Due to the local nature of the blocks, global information is easily lost. Different compensation strategies have been proposed, and most existing methods are based on the combination of different sparse attention mechanisms. CSWin [21] introduces two different cross-shaped sliding windows in two parallel attention heads and combines the attention results of two heads to reduce global information loss. Some methods use several fixed-step or randomly selected tokens to introduce long-range dependencies [25, 27]. Reformer [28] proposes a locality-sensitive-hashing (LSH) algorithm for selecting tokens to perform sparse attention, while the explicit sparse transformer [23] proposes top-*k* selective attention. NSA [29] combines compressed attention, top-*k* selective attention, and sliding window-based attention to propose a hierarchical sparse attention mechanism to obtain different levels of information. Unlike these hierarchical sparse attention mechanisms, ELFATT [18] proposes a hybrid head architecture which combines simple sparse blockify attention with global kernelized linear attention in two parallel heads to obtain global information. XAttention [38] uses the sum of antidiagonal values of the attention matrix to select blocks for a further sparse attention computation within these blocks.

This work is significantly different from the above sparse attention mechanisms. DuSA introduces a novel dual-stage sparse attention mechanism design as shown in Fig. 1. The first stage (intrablock sparse attention) is used to obtain intrablock information (local inductive biases) and the second stage (interblock sparse attention) is used to aggregate all blocks according to their similarities (attention scores) to obtain interblock information (long-range dependencies). Hence, DuSA can approximate VSA with a low error. Both stages have low computational complexity and are compatible with memory efficient methods, which can be further accelerated. As an enhanced alternative for basic sparse attention, DuSA can further improve and accelerate some advanced sparse attention mechanisms.

3 Methods

3.1 Vanilla scaled-dot product attention

For an input embedding matrix $\boldsymbol{H} \in \mathbb{R}^{m\times c}$, after three linear transformations, we can obtain the following,

$$\boldsymbol{Q} = \boldsymbol{H}\mathcal{W}_Q, \quad \boldsymbol{K} = \boldsymbol{H}\mathcal{W}_K, \quad \boldsymbol{V} = \boldsymbol{H}\mathcal{W}_V, \tag{1}$$

where $\mathcal{W}_Q \in \mathbb{R}^{c\times c}$, $\mathcal{W}_K \in \mathbb{R}^{c\times c}$, and $\mathcal{W}_V \in \mathbb{R}^{c\times c}$ are three scaling transformation matrices, $\boldsymbol{Q} \in \mathbb{R}^{m\times c}$, $\boldsymbol{K} \in \mathbb{R}^{m\times c}$, and $\boldsymbol{V} \in \mathbb{R}^{m\times c}$ are the query matrix, key matrix, and value matrix, respectively. Vanilla scaled-dot product attention (VSA) obtains the attention matrix $\boldsymbol{A} \in \mathbb{R}^{m\times m}$ and the updated embedding matrix $\boldsymbol{H}$ as follows,

$$\boldsymbol{A} = \mathrm{softmax}\left(\frac{\boldsymbol{Q}\boldsymbol{K}^\top}{\sqrt{c}}\right), \quad \boldsymbol{H} \leftarrow \boldsymbol{A}\boldsymbol{V}. \tag{2}$$

Since $m \gg c$, the softmax operation for the scaled-dot product of $\boldsymbol{Q}$ and $\boldsymbol{K}$ makes VSA quadratic computational complexity with respect to m and becomes the main bottleneck of efficiency.

3.2 Dual-stage sparse attention

Dual-Stage Sparse Attention (DuSA) can be expressed as a two-stage sparse attention process as Figs. 2 and 3 show. In the first stage, DuSA performs local attention (intrablock sparse attention) within each block as follows,

$$\boldsymbol{A}_1 = \mathrm{softmax}\left(\frac{\boldsymbol{Q}\boldsymbol{K}^\top}{\sqrt{c}} \odot \boldsymbol{Z}_1\right), \quad \boldsymbol{H}_1 \leftarrow \boldsymbol{A}_1\boldsymbol{V}, \tag{3}$$

where $\odot$ denotes the Hadamard product [39] and $\boldsymbol{Z}_1 = \boldsymbol{D}_{(m/b)} \otimes \boldsymbol{U}_{(b)}$ with $\otimes$ denoting the Kronecker product [39], b being the block size, $\boldsymbol{D}_{(m/b)} \in \mathbb{R}^{(m/b)\times(m/b)}$ being a matrix of which diagonal elements are 1 and all the other elements are $-\infty$, and $\boldsymbol{U}_{(b)} \in \mathbb{R}^{b\times b}$ being the all-ones matrix.

Before considering the second stage of DuSA, we need to consider the mathematical expressions for blockify Strategies 1 and 2 in Figs. 2 and 3.

Remark 1. Let $\mathbb{J}_j = \{j, j+b, \ldots, j+(m/b-1)b\}$ with $j = 1, 2, \ldots, b$. Hence, for blockify Strategy 1, the matrix $\boldsymbol{Z}_2 \in \mathbb{R}^{m\times m}$ is defined as $\boldsymbol{Z}_2(\mathbb{J}_j, \mathbb{J}_j)$[1]$= \boldsymbol{U}_{(m/b)}$ with $j = 1, 2, \ldots, b$, and all the other elements of $\boldsymbol{Z}_2$ are $-\infty$. Therefore, one has

$$\boldsymbol{A}' = \mathrm{softmax}\left(\frac{\boldsymbol{Q}\boldsymbol{K}^\top}{\sqrt{c}} \odot \boldsymbol{Z}_2\right), \quad \boldsymbol{H}' \leftarrow \boldsymbol{A}'\boldsymbol{H}_1. \tag{4}$$

Remark 2. We also introduce several notations (rolling indices) as follows:

$$\begin{aligned}
\{\mathbb{J}_1^{(1)}, \mathbb{J}_2^{(1)}, \ldots, \mathbb{J}_{b-1}^{(1)}, \mathbb{J}_b^{(1)}\} &= \{\mathbb{J}_1, \mathbb{J}_2, \ldots, \mathbb{J}_b\},\\
\{\mathbb{J}_1^{(2)}, \mathbb{J}_2^{(2)}, \ldots, \mathbb{J}_{b-1}^{(2)}, \mathbb{J}_b^{(2)}\} &= \{\mathbb{J}_2, \ldots, \mathbb{J}_b, \mathbb{J}_1\},\\
&\cdots\\
\{\mathbb{J}_1^{(b)}, \mathbb{J}_2^{(b)}, \ldots, \mathbb{J}_{b-1}^{(b)}, \mathbb{J}_b^{(b)}\} &= \{\mathbb{J}_b, \mathbb{J}_1, \ldots, \mathbb{J}_{b-1}\}.
\end{aligned}$$

For each k, the matrix $\boldsymbol{A}_k''$ is defined as $\boldsymbol{A}_k''(\mathbb{J}_j, \mathbb{J}_j) = \boldsymbol{A}(\mathbb{J}_j^{(k)}, \mathbb{J}_j^{(k)})$ with $j = 1, 2, \ldots, b$, and $\boldsymbol{A}_k''(\mathbb{J}_j, \mathbb{J}_{j'}) = \boldsymbol{0}_{(m/b)}$ with $\boldsymbol{0}_{(m/b)} \in \mathbb{R}^{(m/b)\times(m/b)}$ being the all-zeros matrix and $j \neq j'$. Note that $\boldsymbol{A}_1'' = \boldsymbol{A}'$. Therefore, for blockify Strategy 2, we have

$$\boldsymbol{A}'' = \sum_{k=1}^{b} \boldsymbol{A}_k'', \quad \boldsymbol{H}'' \leftarrow \boldsymbol{A}''\boldsymbol{H}_1. \tag{5}$$

The upper bounds of Eqs. (3-5) are discussed in Section A1 in Appendix. Based on Remarks 1 and 2, the second stage of DuSA performs interblock sparse attention as follows,

$$\boldsymbol{A}_2 = \boldsymbol{A}'', \quad \boldsymbol{H}_2 \leftarrow \boldsymbol{H}'' = \boldsymbol{A}''\boldsymbol{H}_1 = \boldsymbol{A}_2(\boldsymbol{A}_1\boldsymbol{V}), \tag{6}$$

or

$$\boldsymbol{A}_2 = \boldsymbol{A}', \quad \boldsymbol{H}_2 \leftarrow \boldsymbol{H}' = \boldsymbol{A}'\boldsymbol{H}_1 = \boldsymbol{A}_2(\boldsymbol{A}_1\boldsymbol{V}). \tag{7}$$

4 Experiments and results

4.1 Experiment settings

DuSA is evaluated in image classification (ImageNet-1K [40]), long range arena (LRA [41]), text to video generation (Open-Sora 2.0 [42] prompt sets[2]), semantic segmentation (ADE20K [43]), object detection (MS COCO 2017 [44]), and long context understanding (LongBench [45]) tasks. DuSA0 denotes DuSA (without using Strategies 1 and 2), DuSA1 denotes DuSA (Strategy 1), and DuSA2 denotes DuSA (Strategy 2). If not specified, all results of DuSA were obtained using DuSA2. For image classification, semantic segmentation, and object detection tasks, we compared DuSA with Agent [16], cross-shaped sliding window attention (CSW) [21], EFFATT [15], ELFATT [18], FA2 [5], FLatten [7], sliding window attention (SW) [20], and VSA [1]. The ViT backbones used for image classification, semantic segmentation, and object detection tasks are: CSWin-T/B [7, 21] and Swin-T/B [20]. The original backbones using CSW or SW are named with the suffix "LOCAL": CSWin-T/B-LOCAL and Swin-T/B-LOCAL. The naming scheme for backbones using other attention mechanisms to replace CSW or SW is to add the corresponding attention mechanism name as a suffix after the backbone name, for example, CSWin-T-DuSA. We followed the training protocol of [18, 21, 46] to adopt the same training settings and data augmentation methods to train all methods. Some advanced non-ViT architectures: ConvNeXt-T [47] and VMamba-T [46] are selected for comparison. The experiments were conducted using 8 NVIDIA vGPU (32GB) GPUs. For LRA, we compared DuSA with FA2, Linformer [22], Nyströmformer [3], Primal [36], Reformer [28], and VSA. We followed the training protocol and the settings of [18, 36] and performed the experiments using 1

[1]For a given matrix $\boldsymbol{B} \in \mathbb{R}^{m\times n}$, and two index sets $\mathbb{I} = \{i_1, \ldots, i_s\} \subset \{1, 2, \ldots, m\}$ with $1 \leq i_1 < \cdots < i_s \leq m$ and $\mathbb{J} = \{j_1, \ldots, j_t\} \subset \{1, 2, \ldots, n\}$ with $1 \leq j_1 < \cdots < j_t \leq n$, we let $\boldsymbol{B}(\mathbb{I}, \mathbb{J})$ denote the submatrix $\in \mathbb{R}^{s\times t}$ of $\boldsymbol{B}$ with entries $\{b_{ij}\}_{i\in\mathbb{I}, j\in\mathbb{J}}$.

[2]https://github.com/hpcaitech/Open-Sora/blob/main/assets/texts

NVIDIA A100 (40GB) GPU. We followed the settings of [30] to run text to video generation using DuSA. The backbone used is CogVideoX-2B [48]. We compared DuSA with FA2 and SpargeAttn [30]. Complexity analysis, the ablation study about different block sizes, and more experiments (plug and play examples, the use of DuSA in vanilla ViT architectures [49], memory consumption patterns, and the comparison of DuSA with FlashAttention of FlashInfer [50] and XAttention [38] in accelerating the prefilling stage of Llama-3.1-8B-Instruct [51] on LongBench) are available in Appendix. The source code of DuSA is available in Supplementary Material. For ImageNet-1K, ADE20K and MS COCO 2017, all methods including DuSA that are compatible with FA2, are accelerated by FA2. For text to video generation, DuSA is further accelerated by SpargeAttn.

Table 1: The test accuracy comparison of different methods on LRA. The best values are in bold.

Dataset (sequence length)	Linformer	Nyströmformer	Primal	Reformer	VSA	DuSA
ListOps (2K)	37.3	37.2	37.3	19.1	37.1	**38.1**
Text (4K)	55.9	**65.5**	61.2	64.9	65.0	65.3
Retrieval (4K)	79.4	79.6	77.8	78.6	79.4	**81.4**
Image (1K)	37.8	41.6	43.0	**43.3**	38.2	42.7
Pathfinder (1K)	67.6	70.9	68.3	69.4	**74.2**	73.3
Average accuracy (%)	55.6	59.0	57.5	55.1	58.8	**60.2**

Table 2: The comparison of running time (s) per 1K training steps and peak memory consumption of different methods on LRA using 1 NVIDIA H20 (96GB) GPU.

Dataset (sequence length)	FA2	Linformer	Nyströmformer	Primal	Reformer	VSA	DuSA
	Time (s) | Memory (GB)						
ListOps (2K)	24.2 | **0.4**	19.6 | 1.1	28.3 | 0.6	21.2 | 0.5	34.9 | 1.4	71.2 | 4.3	**16.8** | 0.5
Text (4K)	63.7 | **0.8**	35.1 | 2.2	50.4 | 1.2	33.9 | 0.9	69.3 | 2.8	263.2 | 16.5	**30.7** | 1.3
Retrieval (4K)	126.3 | **1.4**	69.1 | 4.1	96.0 | 2.4	66.5 | 1.9	137.8 | 5.4	523.0 | 17.2	**66.1** | 2.2
Image (1K)	48.9 | **0.8**	45.8 | 2.2	69.7 | 1.4	49.8 | 1.0	82.9 | 2.9	109.2 | 4.5	**44.8** | 1.2
Pathfinder (1K)	63.8 | **0.8**	63.4 | 2.2	91.0 | 1.4	64.6 | 1.0	113.5 | 2.9	144.2 | 4.5	**52.2** | 1.1

4.2 Long range arena

DuSA is compared with state-of-the-art attention mechanisms in LRA as Table 1 shows. It can be seen that DuSA achieves state-of-the-art performance in LRA. DuSA significantly outperforms VSA in long hierarchically structured data modeling (ListOps (2K)), text classification (Text (4K)), image classification on sequences of pixels (Image (1K)), and document retrieval (Retrieval (4K)) tasks. Only in long-range spatial dependency learning (Pathfinder (1K)), DuSA is slightly inferior to VSA, but it is significantly better than other efficient attention mechanisms in this task. Furthermore, DuSA is faster than all comparison methods and offers 2.4-8.6× speedups over VSA and 1.1-2.1× speedups over FA2 and achieves the third lowest memory consumption as shown in Table 2.

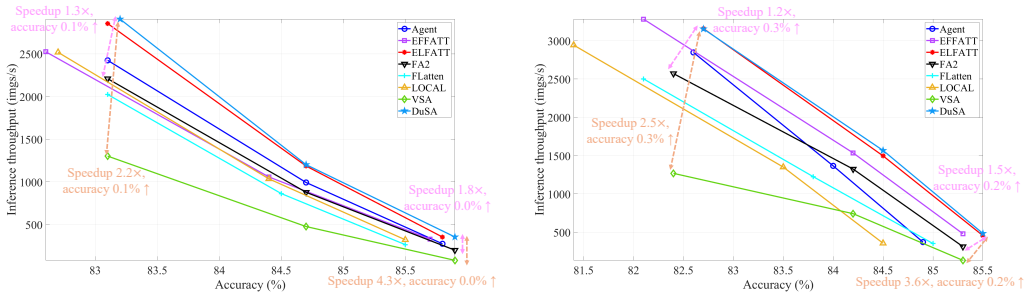

(a) Backbone: CSWin-T/B (b) Backbone: Swin-T/B

Figure 4: Accuracy-efficiency (inference throughput) curves of different methods on ImageNet-1K.

4.3 Image classification performance

Fig. 4 presents a comprehensive performance comparison of various methods in the image classification task (ImageNet-1K). The experimental results demonstrate that DuSA achieves superior

classification accuracy compared to all methods in different model sizes and input resolutions. In addition, DuSA is faster than all comparison methods and offers 2.2-4.3× speedups over VSA and 1.2-1.8× speedups over FA2 using CSWin/Swin backbones. More detailed results can be found in Table A1 in Appendix. Fig. 5 shows the visual comparison of class activation maps (CAMs) of DuSA, ELFATT, and VSA. Compared to ELFATT and VSA, CAMs of DuSA (Strategy 2) are more accurate than theirs. DuSA2 focuses on the groudtruth objects more accurately than DuSA0/DuSA1.

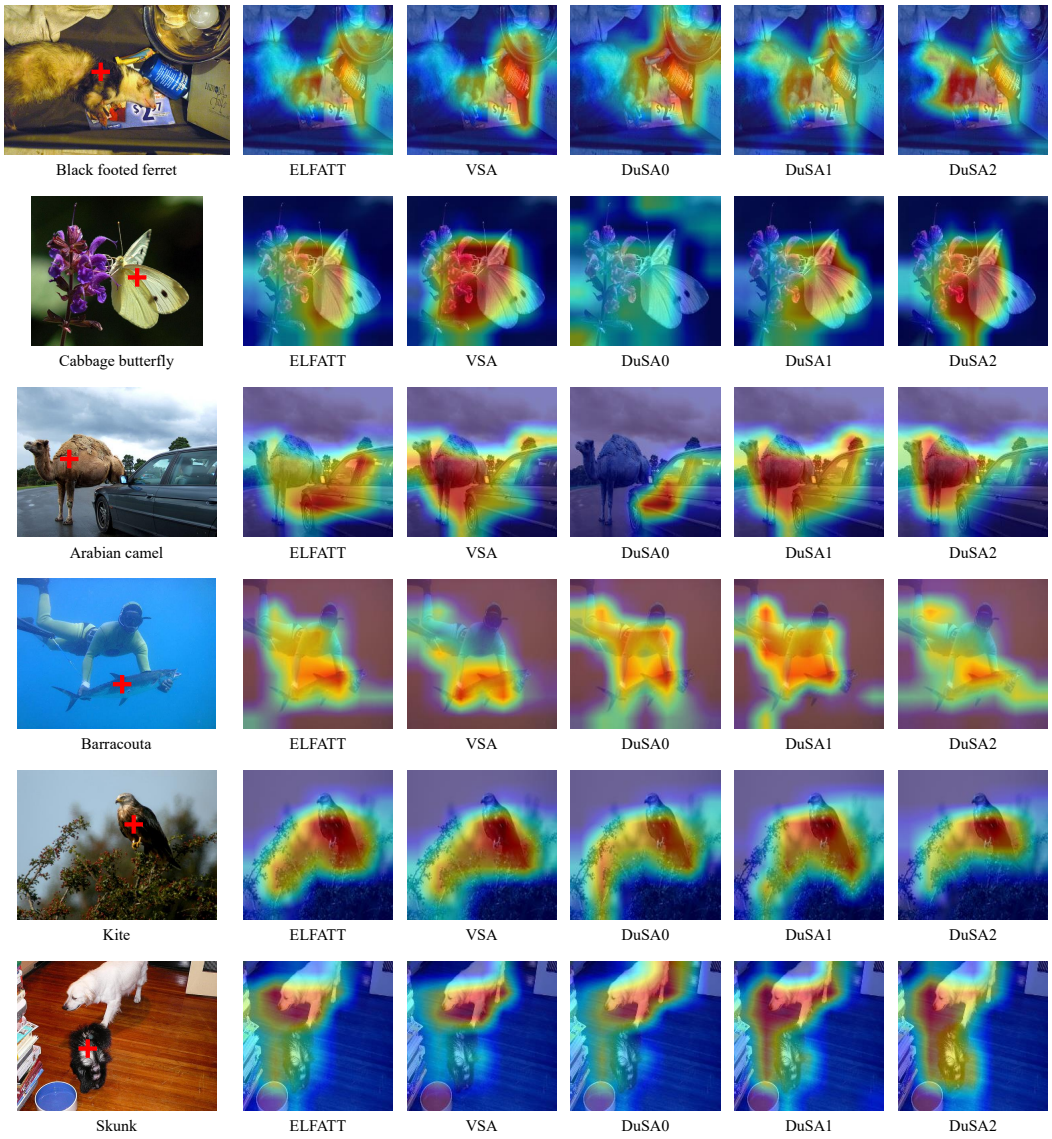

Figure 5: Class activation maps (CAMs) comparison of CSWin-T-DuSA, CSWin-T-ELFATT, and CSWin-T-VSA using Score-CAM [52]. Note: CAMs obtained by DuSA2 and DuSA1 focus on the groudtruth objects more accurately than those of DuSA0 which further demonstrates the effectiveness of the dual-stage spase attention design. In most cases, CAMs of DuSA2 cover more area of the groudtruth objects and less area of the background than those of DuSA1. Compared to ELFATT and VSA, CAMs of DuSA2 are even more accurate than theirs.

4.4 Semantic segmentation performance

Table 3 presents a comprehensive performance comparison of various methods on ADE20K. DuSA significantly outperforms all comparison methods in terms of mean class accuracy (mAcc) and mean intersection over union (mIoU). As for inference speed, DuSA matches the speed of some extremely

Table 3: ADE20K semantic segmentation comparison. Note: Number of floating point operations (FLOPs) are based on an input size of 512×2048. # is parameter numbers.

UperNet [53] using 160K fine-tuning iterations. Inference throughput (FPS) was measured on 1 NVIDIA H20 with a batch size of 1 and mixed precision.					
Method	mAcc	mIoU	FPS (imgs/s)	#	FLOPs
			CSWin-T | Swin-T		
Agent	60.8 | 58.5	48.5 | 46.7	17 | 4	50M | 61M	929.64G | 957.50G
EFFATT	60.6 | 58.3	48.8 | 46.7	33 | 39	50M | 60M	930.34G | 939.35G
ELFATT	61.2 | 59.3	**49.6** | 47.7	32 | 38	50M | 62M	929.53G | 943.94G
FLatten	**61.4** | 57.0	49.3 | 44.8	27 | 35	51M | 61M	930.19G | 944.62G
LOCAL	61.1 | 55.6	**49.6** | 44.5	28 | 38	50M | 60M	928.68G | 945.66G
VSA	61.1 | 59.3	48.8 | 47.8	6/14 (FA2) | 5/14 (FA2)	50M | 60M	2458.75G/928.67G (FA2) | 2873.79G/937.84G (FA2)
DuSA	**61.4** | **59.8**	**49.6** | **48.0**	32 | 37	50M | 62M	928.69G | 942.98G
			Others		
ConvNeXt-T	58.3	46.1	37	60M	939.69G
VMamba-T	59.3	47.9	34	62M	948.78G

fast methods: EFFATT and ELFATT, and offers 5.3-7.4× speedups over VSA and 2.3-2.6× speedups over FA2. Both backbones using DuSA significantly outperform ConvNeXt-T and VMamba-T. Swin-T-DuSA is as fast as ConvNeXt-T and faster than VMamba-T in semantic segmentation.

4.5 Object detection performance

Table 4 compares the object detection performance of various methods on MS COCO 2017. DuSA matches the state-of-the-art performance of ELFATT and significantly outperforms other attention mechanisms with higher box/mask average precision (AP^b/AP^m) in both '1×' fine-tuning training schedule and '3×' multiscale (MS) fine-tuning training schedule. DuSA offers 5.6-8.3× speedups over VSA and 2.2-2.9× speedups over FA2. CSWin-T-DuSA significantly outperforms VMamba-T in object detection with higher box/mask average precision and faster speed. Swin-T-DuSA also significantly outperforms ConvNeXt-T in terms of both performance and speed.

Table 4: MS COCO 2017 object detection comparison. Note: FLOPs are based on an input size of 1280×800. FPS was measured on 1 NVIDIA H20 with a batch size of 1 and mixed precision.

Mask R-CNN [54] 1× schedule | 3×MS schedule									
Method	AP^b	AP^b_{50}	AP^b_{75}	AP^m	AP^m_{50}	AP^m_{75}	FPS (imgs/s)	#	GFLOPs
				CSWin-T					
Agent	46.8 | 49.3	68.9 | 70.8	51.3 | 53.9	42.3 | 43.9	65.9 | 67.9	45.3 | 47.3	20	40M	254.51
EFFATT	46.1 | 48.5	68.3 | 70.0	50.5 | 53.2	41.9 | 43.4	65.5 | 67.3	45.3 | 46.9	36	40M	255.20
ELFATT	**47.0** | **49.4**	**69.2** | **70.9**	51.4 | **54.4**	42.6 | 44.0	**66.4** | **68.0**	**45.9** | 47.5	33	40M	254.40
FLatten	46.6 | 48.9	68.8 | 70.8	51.0 | 53.5	42.2 | 43.9	65.7 | 67.9	45.3 | 47.3	28	41M	255.05
LOCAL	46.5 | 49.3	68.5 | 70.8	51.0 | 54.3	42.1 | 44.0	65.6 | 67.8	45.3 | 47.5	28	40M	253.57
VSA	**47.0** | 48.8	69.1 | 70.0	**51.9** | 53.5	42.6 | 43.6	66.1 | 67.4	**45.9** | 47.1	7/18 (FA2)	40M	1712.76/253.56 (FA2)
DuSA	46.9 | **49.4**	**69.2** | **70.9**	51.7 | **54.4**	**42.7** | **44.1**	**66.4** | 67.8	**45.9** | **47.6**	39	40M	253.58
				Swin-T					
Agent	44.6 | 47.3	67.5 | 69.5	48.7 | 51.9	40.7 | 42.7	64.4 | 66.4	43.4 | 46.2	5	48M	278.42
EFFATT	44.7 | 47.6	67.0 | 69.4	48.9 | 52.6	41.1 | 42.7	64.0 | 65.9	44.4 | 46.1	46	48M	261.95
ELFATT	**46.1** | **48.5**	**68.3** | **70.4**	50.8 | **53.4**	42.1 | 43.6	**65.4** | 67.3	45.3 | 47.3	45	50M	266.43
FLatten	44.2 | 46.5	67.3 | 68.5	48.5 | 50.8	40.2 | 42.1	63.8 | 65.4	43.0 | 45.1	41	49M	266.43
LOCAL	42.7 | 46.0	65.2 | 68.1	46.8 | 50.3	39.3 | 41.6	62.2 | 65.1	42.2 | 44.9	45	48M	267.01
VSA	45.4 | 48.0	67.9 | 70.0	49.7 | 52.7	41.6 | 43.3	65.0 | 67.0	44.8 | 46.8	6/17 (FA2)	48M	2106.75/260.48 (FA2)
DuSA	46.0 | 48.4	68.2 | 70.3	**50.9** | 53.0	**42.2** | **43.8**	65.3 | **67.5**	**45.5** | **47.5**	50	50M	265.50
				Other tiny models					
ConvNeXt	44.2 | 46.2	66.6 | 67.9	48.3 | 50.8	40.1 | 41.7	63.3 | 65.0	42.8 | 44.9	44	48M	262.29
VMamba	47.4 | 48.9	69.5 | 70.6	52.0 | 53.6	42.7 | 43.7	66.3 | 67.7	46.0 | 46.8	35	50M	271.16

Table 5: The comparison of text to video generation using CogVideoX-2B (sequence length: 17K) as the backbone. Note: The speed metric, TOPS (tera operations per second) [30], is the attention kernel speed. The speed was obtained using 1 NVIDIA vGPU (32GB) with BF16 precision.

Method	TOPS ↑	CLIPSIM ↑	CLIP-T ↑	VQA-a ↑	VQA-t ↑	Flow-score ↑
FA2	103	0.2022	**0.9971**	**51.6921**	**48.3386**	5.6719
SpargeAttn (sparsity: 0.46)	198	0.2015	0.9968	51.5676	48.2785	5.7631
DuSA (sparsity: 0.50)	**258**	**0.2024**	0.9966	51.6049	48.3379	**6.0482**

(a) FA2 (CLIPSIM: 0.2161, CLIP-T: 0.9983, VQA-a: 53.4576, VQA-t: 48.9721, Flow-score: 12.3805)

(b) SpargeAttn (CLIPSIM: 0.2109, CLIP-T: 0.9984, VQA-a: 52.9862, VQA-t: 48.3282, Flow-score: 10.4248)

(c) DuSA (CLIPSIM: 0.2108, CLIP-T: 0.9986, VQA-a: 53.5017, VQA-t: 48.7888, Flow-score: 8.7635)

Figure 6: DuSA achieves noninferior video generation quality compared to VSA using FA2 for acceleration and outperforms SpargeAttn.

(a) FA2 (CLIPSIM: 0.1955, CLIP-T: 0.9992, VQA-a: 54.6491, VQA-t: 49.1951, Flow-score: 6.6526)

(b) SpargeAttn (CLIPSIM: 0.2044, CLIP-T: 0.9991, VQA-a: 53.2634, VQA-t: 48.8170, Flow-score: 6.1444)

(c) DuSA (CLIPSIM: 0.2065, CLIP-T: 0.9982, VQA-a: 53.5948, VQA-t: 49.1732, Flow-score: 6.7921)

Figure 7: DuSA achieves noninferior video generation quality compared to VSA using FA2 for acceleration and outperforms SpargeAttn.

4.6 Text to video generation performance

Table 5 compares DuSA, FA2, and SpargeAttn in text to video generation (Open-Sora 2.0 prompt sets) using CogVideoX-2B as the backbone. We followed [30] to use CLIPSIM [55], CLIP-T [55], VQA-a [56], VQA-t [56], and Flow-score [57] to evaluate text-video alignment, aesthetic and technical quality of the video, and temporal consistency. Using a similar sparsity ratio, DuSA obtains better text-video alignment (CLIPSIM), higher video aesthetic and technical quality (VQA-a and VQA-t), and better temporal consistency (Flow-score) than SpargeAttn and its performance is almost at the same level compared to VSA using FA2 for acceleration. DuSA is faster than FA2 and SpargeAttn using BF16 precision. DuSA uses 98s, while FA2 uses 147s and SpargeAttn uses 106s on 1 NVIDIA vGPU (32GB) with BF16 precision for end-to-end generation. Figs. 6 and 7 show the visual comparison of DuSA, SpargeAttn, and VSA (FA2) in text to video generation. DuSA achieves better video generation quality than SpargeAttn and noninferior quality compared to VSA.

Table 6: Effect of different blockify strategies or stage execution orders of DuSA on ImageNet-1K. Note: FPS was measured on 1 NVIDIA H20 using a batch size of 512 and mixed precision.

Method	Resolution	Accuracy (%)	FPS (imgs/s)	#	FLOPs
CSWin-T					
DuSA0	224^2	82.9	3197	20M	4.09G
DuSA1 (1^{st}: Intrablock; 2^{nd}: Interblock)	224^2	83.0	2909	20M	4.09G
DuSA1 (1^{st}: Interblock; 2^{nd}: Intrablock)	224^2	82.9	2880	20M	4.09G
DuSA2 (1^{st}: Intrablock; 2^{nd}: Interblock)	224^2	83.2	2908	20M	4.09G
DuSA2 (1^{st}: Interblock; 2^{nd}: Intrablock)	224^2	83.0	2866	20M	4.09G
Swin-T					
DuSA0	224^2	82.5	3481	30M	4.63G
DuSA1 (1^{st}: Intrablock; 2^{nd}: Interblock)	224^2	82.6	3136	30M	4.63G
DuSA1 (1^{st}: Interblock; 2^{nd}: Intrablock)	224^2	82.6	3095	30M	4.63G
DuSA2 (1^{st}: Intrablock; 2^{nd}: Interblock)	224^2	82.7	3154	30M	4.63G
DuSA2 (1^{st}: Interblock; 2^{nd}: Intrablock)	224^2	82.6	3062	30M	4.63G

4.7 Ablation studies about different blockify strategies and different stage execution orders

Table 6 shows the comparison of DuSA using different blockify strategies on ImageNet-1K. Without using any blockify strategies, the speed is the fastest; however, its performance is also the lowest. Strategy 2 (DuSA2) obtains the highest accuracy because it includes more token information for each token in token mixing, as Fig. 3 shows. And its speed is almost the same as that of Strategy 1. Additionally, as illustrated in the visual comparison of Fig. 5, CAMs obtained using Strategies 1 and 2 focus more accurately on the ground-truth objects than those obtained without using Strategies 1 and 2, further demonstrating the effectiveness of the dual-stage sparse attention design. In most cases, CAMs of Strategy 2 cover more area of the groudtruth objects and less area of the background than those of Strategy 1. Table 6 also shows the comparison of DuSA using different execution orders of two stages on ImageNet-1K. Due to the change in execution order, the speed is slightly different due to the different reshaping operations and convolutions for different value matrices used for position encoding. Performing intrablock sparse attention first usually outperforms performing interblock sparse attention first in terms of both speed and accuracy.

5 Conclusions

In this paper, we propose DuSA for attention acceleration of transformers. DuSA further advances single-stage sparse attention mechanisms through the novel dual-stage sparse attention mechanism design. Both stages are designed to have low computational complexity and can be further accelerated by memory acceleration methods. The dual-stage sparse attention design provides a lower error in approximating vanilla scaled-dot product attention than the basic single-stage sparse attention mechanisms. DuSA can still maintain low performance loss in some plug and play situations. DuSA can be used in both training and inference acceleration. After training, DuSA can even outperform VSA. DuSA achieves state-of-the-art performance in different benchmarks: long range arena, image classification, semantic segmentation, object detection, text to video generation, and long context understanding, and accelerates models of different sizes.

Acknowledgements

This work is supported by the Hong Kong Innovation and Technology Commission (InnoHK Project CIMDA), the Institute of Digital Medicine, City University of Hong Kong (Projects 9229503 and 9610460), the National Natural Science Foundation of China (No. 12561095), and the Special Posts of Guizhou University (No. [2025]06).

References

[1] A. Vaswani, N. Shazeer, N. Parmar, J. Uszkoreit, L. Jones, A. N. Gomez, Ł. Kaiser, and I. Polosukhin, "Attention is all you need," in *Advances in Neural Information Processing Systems*, I. Guyon, U. V. Luxburg, S. Bengio, H. Wallach, R. Fergus, S. Vishwanathan, and R. Garnett, Eds., vol. 30. Curran Associates, Inc., 2017, pp. 5998–6008.

[2] J. Han, L. Zeng, L. Du, X. Ye, W. Ding, and J. Feng, "Modify self-attention via skeleton decomposition for effective point cloud transformer," in *Proceedings of the AAAI Conference on Artificial Intelligence*, vol. 36, no. 1, 2022, pp. 808–816.

[3] Y. Xiong, Z. Zeng, R. Chakraborty, M. Tan, G. Fung, Y. Li, and V. Singh, "Nyströmformer: A Nyström-based algorithm for approximating self-attention," in *Proceedings of the AAAI Conference on Artificial Intelligence*, vol. 35, no. 16, 2021, pp. 14 138–14 148.

[4] T. Dao, D. Fu, S. Ermon, A. Rudra, and C. Ré, "FlashAttention: Fast and memory-efficient exact attention with IO-awareness," in *Advances in Neural Information Processing Systems*, S. Koyejo, S. Mohamed, A. Agarwal, D. Belgrave, K. Cho, and A. Oh, Eds., vol. 35. Curran Associates, Inc., 2022, pp. 16 344–16 359.

[5] T. Dao, "FlashAttention-2: Faster attention with better parallelism and work partitioning," in *International Conference on Learning Representations*, 2024. [Online]. Available: https://openreview.net/forum?id=mZn2Xyh9Ec

[6] J. Shah, G. Bikshandi, Y. Zhang, V. Thakkar, P. Ramani, and T. Dao, "FlashAttention-3: Fast and accurate attention with asynchrony and low-precision," in *Advances in Neural Information Processing Systems*, A. Globerson, L. Mackey, D. Belgrave, A. Fan, U. Paquet, J. Tomczak, and C. Zhang, Eds., vol. 37. Curran Associates, Inc., 2024, pp. 68 658–68 685.

[7] D. Han, X. Pan, Y. Han, S. Song, and G. Huang, "FLatten transformer: Vision transformer using focused linear attention," in *Proceedings of the IEEE/CVF International Conference on Computer Vision (ICCV)*, 2023, pp. 5961–5971.

[8] K. M. Choromanski, V. Likhosherstov, D. Dohan, X. Song, A. Gane, T. Sarlos, P. Hawkins, J. Q. Davis, A. Mohiuddin, Ł. Kaiser, D. B. Belanger, L. J. Colwell, and A. Weller, "Rethinking attention with performers," in *International Conference on Learning Representations*, 2021. [Online]. Available: https://openreview.net/forum?id=Ua6zuk0WRH

[9] M. Wortsman, J. Lee, J. Gilmer, and S. Kornblith, "Replacing softmax with ReLU in vision transformers," *arXiv preprint arXiv:2309.08586*, 2023.

[10] A. Katharopoulos, A. Vyas, N. Pappas, and F. Fleuret, "Transformers are RNNs: Fast autoregressive transformers with linear attention," in *Proceedings of the 37th International Conference on Machine Learning*, ser. Proceedings of Machine Learning Research, H. D. III and A. Singh, Eds., vol. 119. PMLR, 2020, pp. 5156–5165. [Online]. Available: https://proceedings.mlr.press/v119/katharopoulos20a.html

[11] D. Bolya, C.-Y. Fu, X. Dai, P. Zhang, and J. Hoffman, "Hydra attention: Efficient attention with many heads," in *Computer Vision – ECCV 2022 Workshops*, L. Karlinsky, T. Michaeli, and K. Nishino, Eds. Cham: Springer Nature Switzerland, 2023, pp. 35–49.

[12] J. Lu, J. Yao, J. Zhang, X. Zhu, H. Xu, W. Gao, C. Xu, T. Xiang, and L. Zhang, "SOFT: Softmax-free transformer with linear complexity," in *Advances in Neural Information Processing Systems*, M. Ranzato, A. Beygelzimer, Y. Dauphin, P. Liang, and J. W. Vaughan, Eds., vol. 34. Curran Associates, Inc., 2021, pp. 21 297–21 309.

[13] H. Peng, N. Pappas, D. Yogatama, R. Schwartz, N. Smith, and L. Kong, "Random feature attention," in *International Conference on Learning Representations*, 2021. [Online]. Available: https://openreview.net/forum?id=QtTKTdVrFBB

[14] Z. Qin, W. Sun, H. Deng, D. Li, Y. Wei, B. Lv, J. Yan, L. Kong, and Y. Zhong, "cosFormer: Rethinking softmax in attention," in *International Conference on Learning Representations*, 2022. [Online]. Available: https://openreview.net/forum?id=Bl8CQrx2Up4

[15] Z. Shen, M. Zhang, H. Zhao, S. Yi, and H. Li, "Efficient attention: Attention with linear complexities," in *Proceedings of the IEEE/CVF Winter Conference on Applications of Computer Vision (WACV)*, 2021, pp. 3531–3539.

[16] D. Han, T. Ye, Y. Han, Z. Xia, S. Pan, P. Wan, S. Song, and G. Huang, "Agent attention: On the integration of softmax and linear attention," in *Computer Vision – ECCV 2024*, A. Leonardis, E. Ricci, S. Roth, O. Russakovsky, T. Sattler, and G. Varol, Eds. Cham: Springer Nature Switzerland, 2025, pp. 124–140.

[17] C. Wu, M. Che, and H. Yan, "The CUR decomposition of self-attention matrices in vision transformers," *IEEE Transactions on Pattern Analysis and Machine Intelligence*, 2025. [Online]. Available: https://doi.org/10.1109/TPAMI.2025.3646452

[18] C. Wu, M. Che, R. Xu, Z. Ran, and H. Yan, "ELFATT: Efficient linear fast attention for vision transformers," in *Proceedings of the 33rd ACM International Conference on Multimedia*, ser. MM '25. New York, NY, USA: Association for Computing Machinery, 2025, pp. 9140–9149. [Online]. Available: https://doi.org/10.1145/3746027.3754825

[19] Z. Ran, Z. Ye, C. Wu, R. C. C. Cheung, and H. Yan, "FastViT: Real-time linear attention accelerator for dense predictions of vision transformer (ViT)," in *2025 IEEE International Symposium on Circuits and Systems (ISCAS)*, 2025. [Online]. Available: https://doi.org/10.1109/ISCAS56072.2025.11043624

[20] Z. Liu, Y. Lin, Y. Cao, H. Hu, Y. Wei, Z. Zhang, S. Lin, and B. Guo, "Swin transformer: Hierarchical vision transformer using shifted windows," in *Proceedings of the IEEE/CVF International Conference on Computer Vision (ICCV)*, 2021, pp. 10 012–10 022.

[21] X. Dong, J. Bao, D. Chen, W. Zhang, N. Yu, L. Yuan, D. Chen, and B. Guo, "CSWin transformer: A general vision transformer backbone with cross-shaped windows," in *Proceedings of the IEEE/CVF Conference on Computer Vision and Pattern Recognition (CVPR)*, 2022, pp. 12 124–12 134.

[22] S. Wang, B. Z. Li, M. Khabsa, H. Fang, and H. Ma, "Linformer: Self-attention with linear complexity," *arXiv preprint arXiv:2006.04768*, 2020.

[23] G. Zhao, J. Lin, Z. Zhang, X. Ren, Q. Su, and X. Sun, "Explicit sparse transformer: Concentrated attention through explicit selection," *CoRR*, vol. abs/1912.11637, 2019. [Online]. Available: https://arxiv.org/abs/1912.11637

[24] I. Beltagy, M. E. Peters, and A. Cohan, "Longformer: The long-document transformer," *CoRR*, vol. abs/2004.05150, 2020. [Online]. Available: https://arxiv.org/abs/2004.05150

[25] R. Child, S. Gray, A. Radford, and I. Sutskever, "Generating long sequences with sparse transformers," *CoRR*, vol. abs/1904.10509, 2019. [Online]. Available: https://arxiv.org/abs/1904.10509

[26] Y. Tay, D. Bahri, L. Yang, D. Metzler, and D.-C. Juan, "Sparse Sinkhorn attention," in *Proceedings of the 37th International Conference on Machine Learning*, ser. Proceedings of Machine Learning Research, H. D. III and A. Singh, Eds., vol. 119. PMLR, 2020, pp. 9438–9447. [Online]. Available: https://proceedings.mlr.press/v119/tay20a.html

[27] M. Zaheer, G. Guruganesh, K. A. Dubey, J. Ainslie, C. Alberti, S. Ontanon, P. Pham, A. Ravula, Q. Wang, L. Yang, and A. Ahmed, "Big Bird: Transformers for longer sequences," in *Advances in Neural Information Processing Systems*, H. Larochelle, M. Ranzato, R. Hadsell, M. Balcan, and H. Lin, Eds., vol. 33. Curran Associates, Inc., 2020, pp. 17 283–17 297.

[28] N. Kitaev, Ł. Kaiser, and A. Levskaya, "Reformer: The efficient transformer," in *International Conference on Learning Representations*, 2020. [Online]. Available: https://openreview.net/forum?id=rkgNKkHtvB

[29] J. Yuan, H. Gao, D. Dai, J. Luo, L. Zhao, Z. Zhang, Z. Xie, Y. Wei, L. Wang, Z. Xiao, Y. Wang, C. Ruan, M. Zhang, W. Liang, and W. Zeng, "Native sparse attention: Hardware-aligned and natively trainable sparse attention," in *Proceedings of the 63rd Annual Meeting of the Association for Computational Linguistics (Volume 1: Long Papers)*, W. Che, J. Nabende, E. Shutova, and M. T. Pilehvar, Eds. Association for Computational Linguistics, 2025, pp. 23 078–23 097. [Online]. Available: https://aclanthology.org/2025.acl-long.1126/

[30] J. Zhang, C. Xiang, H. Huang, J. Wei, H. Xi, J. Zhu, and J. Chen, "SpargeAttention: Accurate and training-free sparse attention accelerating any model inference," in *Proceedings of the 42nd International Conference on Machine Learning*, ser. Proceedings of Machine Learning Research, A. Singh, M. Fazel, D. Hsu, S. Lacoste-Julien, F. Berkenkamp, T. Maharaj, K. Wagstaff, and J. Zhu, Eds., vol. 267. PMLR, 2025, pp. 76 397–76 413. [Online]. Available: https://proceedings.mlr.press/v267/zhang25ch.html

[31] J. Ramapuram, F. Danieli, E. G. Dhekane, F. Weers, D. Busbridge, P. Ablin, T. Likhomanenko, J. Digani, Z. Gu, A. Shidani, and R. Webb, "Theory, analysis, and best practices for sigmoid self-attention," in *International Conference on Learning Representations*, 2025. [Online]. Available: https://openreview.net/forum?id=Zhdhg6n2OG

[32] V. Nair and G. E. Hinton, "Rectified linear units improve restricted Boltzmann machines," in *Proceedings of the 27th International Conference on Machine Learning*, ser. ICML'10, J. Fürnkranz and T. Joachims, Eds. Madison, WI, USA: Omnipress, 2010, pp. 807–814.

[33] H. Cai, J. Li, M. Hu, C. Gan, and S. Han, "EfficientViT: Lightweight multi-scale attention for high-resolution dense prediction," in *Proceedings of the IEEE/CVF International Conference on Computer Vision (ICCV)*, 2023, pp. 17 302–17 313.

[34] D.-A. Clevert, T. Unterthiner, and S. Hochreiter, "Fast and accurate deep network learning by exponential linear units (ELUs)," *arXiv preprint arXiv:1511.07289*, 2015.

[35] H. Kang, M.-H. Yang, and J. Ryu, "Interactive multi-head self-attention with linear complexity," *arXiv preprint arXiv:2402.17507*, 2024.

[36] Y. Chen, Q. Tao, F. Tonin, and J. Suykens, "Primal-Attention: Self-attention through asymmetric kernel SVD in primal representation," in *Advances in Neural Information Processing Systems*, A. Oh, T. Naumann, A. Globerson, K. Saenko, M. Hardt, and S. Levine, Eds., vol. 36. Curran Associates, Inc., 2023, pp. 65 088–65 101.

[37] Z. Geng, M.-H. Guo, H. Chen, X. Li, K. Wei, and Z. Lin, "Is attention better than matrix decomposition?" in *International Conference on Learning Representations*, 2021. [Online]. Available: https://openreview.net/forum?id=1FvkSpWosOl

[38] R. Xu, G. Xiao, H. Huang, J. Guo, and S. Han, "XAttention: Block sparse attention with antidiagonal scoring," in *Proceedings of the 42nd International Conference on Machine Learning*, ser. Proceedings of Machine Learning Research, A. Singh, M. Fazel, D. Hsu, S. Lacoste-Julien, F. Berkenkamp, T. Maharaj, K. Wagstaff, and J. Zhu, Eds., vol. 267. PMLR, 2025, pp. 69 819–69 831. [Online]. Available: https://proceedings.mlr.press/v267/xu25ag.html

[39] R. A. Horn and C. R. Johnson, *Matrix Analysis*, 2nd ed. Cambridge University Press, 2012.

[40] O. Russakovsky, J. Deng, H. Su, J. Krause, S. Satheesh, S. Ma, Z. Huang, A. Karpathy, A. Khosla, M. Bernstein, A. C. Berg, and L. Fei-Fei, "ImageNet large scale visual recognition challenge," *International Journal of Computer Vision*, vol. 115, no. 3, pp. 211–252, 2015.

[41] Y. Tay, M. Dehghani, S. Abnar, Y. Shen, D. Bahri, P. Pham, J. Rao, L. Yang, S. Ruder, and D. Metzler, "Long range arena: A benchmark for efficient transformers," in *International Conference on Learning Representations*, 2021. [Online]. Available: https://openreview.net/forum?id=qVyeW-grC2k

[42] X. Peng, Z. Zheng, C. Shen, T. Young, X. Guo, B. Wang, H. Xu, H. Liu, M. Jiang, W. Li *et al.*, "Open-Sora 2.0: Training a commercial-level video generation model in $200K," *arXiv preprint arXiv:2503.09642*, 2025.

[43] B. Zhou, H. Zhao, X. Puig, S. Fidler, A. Barriuso, and A. Torralba, "Scene parsing through ADE20K dataset," in *2017 IEEE Conference on Computer Vision and Pattern Recognition (CVPR)*. Los Alamitos, CA, USA: IEEE Computer Society, 2017, pp. 5122–5130.

[44] T.-Y. Lin, M. Maire, S. Belongie, J. Hays, P. Perona, D. Ramanan, P. Dollár, and C. L. Zitnick, "Microsoft COCO: Common objects in context," in *Computer Vision – ECCV 2014*, D. Fleet, T. Pajdla, B. Schiele, and T. Tuytelaars, Eds. Cham: Springer International Publishing, 2014, pp. 740–755.

[45] Y. Bai, X. Lv, J. Zhang, H. Lyu, J. Tang, Z. Huang, Z. Du, X. Liu, A. Zeng, L. Hou, Y. Dong, J. Tang, and J. Li, "LongBench: A bilingual, multitask benchmark for long context understanding," in *Proceedings of the 62nd Annual Meeting of the Association for Computational Linguistics (Volume 1: Long Papers)*, L.-W. Ku, A. Martins, and V. Srikumar,

Eds. Association for Computational Linguistics, 2024, pp. 3119–3137. [Online]. Available: https://aclanthology.org/2024.acl-long.172/

[46] Y. Liu, Y. Tian, Y. Zhao, H. Yu, L. Xie, Y. Wang, Q. Ye, J. Jiao, and Y. Liu, "VMamba: Visual state space model," in *Advances in Neural Information Processing Systems*, A. Globerson, L. Mackey, D. Belgrave, A. Fan, U. Paquet, J. Tomczak, and C. Zhang, Eds., vol. 37. Curran Associates, Inc., 2024, pp. 103 031–103 063.

[47] Z. Liu, H. Mao, C.-Y. Wu, C. Feichtenhofer, T. Darrell, and S. Xie, "A ConvNet for the 2020s," in *Proceedings of the IEEE/CVF Conference on Computer Vision and Pattern Recognition (CVPR)*, 2022, pp. 11 976–11 986.

[48] Z. Yang, J. Teng, W. Zheng, M. Ding, S. Huang, J. Xu, Y. Yang, W. Hong, X. Zhang, G. Feng, D. Yin, Y. Zhang, W. Wang, Y. Cheng, B. Xu, X. Gu, Y. Dong, and J. Tang, "CogVideoX: Text-to-video diffusion models with an expert transformer," in *International Conference on Learning Representations*, 2025. [Online]. Available: https://openreview.net/forum?id=LQzN6TRFg9

[49] A. Dosovitskiy, L. Beyer, A. Kolesnikov, D. Weissenborn, X. Zhai, T. Unterthiner, M. Dehghani, M. Minderer, G. Heigold, S. Gelly, J. Uszkoreit, and N. Houlsby, "An image is worth 16×16 words: Transformers for image recognition at scale," in *International Conference on Learning Representations*, 2021. [Online]. Available: https://openreview.net/forum?id=YicbFdNTTy

[50] Z. Ye, R. Lai, B.-R. Lu, C.-Y. Lin, S. Zheng, L. Chen, T. Chen, and L. Ceze, "Cascade inference: Memory bandwidth efficient shared prefix batch decoding," February 2024. [Online]. Available: https://flashinfer.ai/2024/02/02/cascade-inference.html

[51] A. Grattafiori, A. Dubey, A. Jauhri, A. Pandey, A. Kadian, A. Al-Dahle, A. Letman, A. Mathur, A. Schelten, A. Vaughan *et al.*, "The Llama 3 herd of models," *arXiv preprint arXiv:2407.21783*, 2024.

[52] H. Wang, Z. Wang, M. Du, F. Yang, Z. Zhang, S. Ding, P. Mardziel, and X. Hu, "Score-CAM: Score-weighted visual explanations for convolutional neural networks," in *2020 IEEE/CVF Conference on Computer Vision and Pattern Recognition Workshops (CVPRW)*. Los Alamitos, CA, USA: IEEE Computer Society, 2020, pp. 111–119.

[53] T. Xiao, Y. Liu, B. Zhou, Y. Jiang, and J. Sun, "Unified perceptual parsing for scene understanding," in *Computer Vision – ECCV 2018*, V. Ferrari, M. Hebert, C. Sminchisescu, and Y. Weiss, Eds. Cham: Springer International Publishing, 2018, pp. 432–448.

[54] K. He, G. Gkioxari, P. Dollár, and R. Girshick, "Mask R-CNN," in *2017 IEEE International Conference on Computer Vision (ICCV)*. Los Alamitos, CA, USA: IEEE Computer Society, 2017, pp. 2980–2988.

[55] Y. Liu, X. Cun, X. Liu, X. Wang, Y. Zhang, H. Chen, Y. Liu, T. Zeng, R. Chan, and Y. Shan, "EvalCrafter: Benchmarking and evaluating large video generation models," in *Proceedings of the IEEE/CVF Conference on Computer Vision and Pattern Recognition (CVPR)*, 2024, pp. 22 139–22 149.

[56] H. Wu, E. Zhang, L. Liao, C. Chen, J. Hou, A. Wang, W. Sun, Q. Yan, and W. Lin, "Exploring video quality assessment on user generated contents from aesthetic and technical perspectives," in *Proceedings of the IEEE/CVF International Conference on Computer Vision (ICCV)*, 2023, pp. 20 144–20 154.

[57] T. Zhao, T. Fang, H. Huang, R. Wan, W. Soedarmadji, E. Liu, S. Li, Z. Lin, G. Dai, S. Yan, H. Yang, X. Ning, and Y. Wang, "ViDiT-Q: Efficient and accurate quantization of diffusion transformers for image and video generation," in *International Conference on Learning Representations*, 2025. [Online]. Available: https://openreview.net/forum?id=E1N1oxd63b

NeurIPS Paper Checklist

1. **Claims**

   Question: Do the main claims made in the abstract and introduction accurately reflect the paper's contributions and scope?

   Answer: [Yes]

   Justification: The main claims made in the abstract and introduction accurately reflect the paper's contributions and scope.

   Guidelines:

   - The answer NA means that the abstract and introduction do not include the claims made in the paper.
   - The abstract and/or introduction should clearly state the claims made, including the contributions made in the paper and important assumptions and limitations. A No or NA answer to this question will not be perceived well by the reviewers.
   - The claims made should match theoretical and experimental results, and reflect how much the results can be expected to generalize to other settings.
   - It is fine to include aspirational goals as motivation as long as it is clear that these goals are not attained by the paper.

2. **Limitations**

   Question: Does the paper discuss the limitations of the work performed by the authors?

   Answer: [Yes]

   Justification: See Section A8 in Appendix.

   Guidelines:

   - The answer NA means that the paper has no limitation while the answer No means that the paper has limitations, but those are not discussed in the paper.
   - The authors are encouraged to create a separate "Limitations" section in their paper.
   - The paper should point out any strong assumptions and how robust the results are to violations of these assumptions (e.g., independence assumptions, noiseless settings, model well-specification, asymptotic approximations only holding locally). The authors should reflect on how these assumptions might be violated in practice and what the implications would be.
   - The authors should reflect on the scope of the claims made, e.g., if the approach was only tested on a few datasets or with a few runs. In general, empirical results often depend on implicit assumptions, which should be articulated.
   - The authors should reflect on the factors that influence the performance of the approach. For example, a facial recognition algorithm may perform poorly when image resolution is low or images are taken in low lighting. Or a speech-to-text system might not be used reliably to provide closed captions for online lectures because it fails to handle technical jargon.
   - The authors should discuss the computational efficiency of the proposed algorithms and how they scale with dataset size.
   - If applicable, the authors should discuss possible limitations of their approach to address problems of privacy and fairness.
   - While the authors might fear that complete honesty about limitations might be used by reviewers as grounds for rejection, a worse outcome might be that reviewers discover limitations that aren't acknowledged in the paper. The authors should use their best judgment and recognize that individual actions in favor of transparency play an important role in developing norms that preserve the integrity of the community. Reviewers will be specifically instructed to not penalize honesty concerning limitations.

3. **Theory assumptions and proofs**

   Question: For each theoretical result, does the paper provide the full set of assumptions and a complete (and correct) proof?

   Answer: [Yes]

Justification: Each theoretical result in Section 3 of the main text and Section A1 of Appendix is provided with a complete (and correct) proof.

Guidelines:

- The answer NA means that the paper does not include theoretical results.
- All the theorems, formulas, and proofs in the paper should be numbered and cross-referenced.
- All assumptions should be clearly stated or referenced in the statement of any theorems.
- The proofs can either appear in the main paper or the supplemental material, but if they appear in the supplemental material, the authors are encouraged to provide a short proof sketch to provide intuition.
- Inversely, any informal proof provided in the core of the paper should be complemented by formal proofs provided in appendix or supplemental material.
- Theorems and Lemmas that the proof relies upon should be properly referenced.

4. **Experimental result reproducibility**

   Question: Does the paper fully disclose all the information needed to reproduce the main experimental results of the paper to the extent that it affects the main claims and/or conclusions of the paper (regardless of whether the code and data are provided or not)?

   Answer: [Yes]

   Justification: See Subsection 4.1.

   Guidelines:

   - The answer NA means that the paper does not include experiments.
   - If the paper includes experiments, a No answer to this question will not be perceived well by the reviewers: Making the paper reproducible is important, regardless of whether the code and data are provided or not.
   - If the contribution is a dataset and/or model, the authors should describe the steps taken to make their results reproducible or verifiable.
   - Depending on the contribution, reproducibility can be accomplished in various ways. For example, if the contribution is a novel architecture, describing the architecture fully might suffice, or if the contribution is a specific model and empirical evaluation, it may be necessary to either make it possible for others to replicate the model with the same dataset, or provide access to the model. In general. releasing code and data is often one good way to accomplish this, but reproducibility can also be provided via detailed instructions for how to replicate the results, access to a hosted model (e.g., in the case of a large language model), releasing of a model checkpoint, or other means that are appropriate to the research performed.
   - While NeurIPS does not require releasing code, the conference does require all submissions to provide some reasonable avenue for reproducibility, which may depend on the nature of the contribution. For example
     (a) If the contribution is primarily a new algorithm, the paper should make it clear how to reproduce that algorithm.
     (b) If the contribution is primarily a new model architecture, the paper should describe the architecture clearly and fully.
     (c) If the contribution is a new model (e.g., a large language model), then there should either be a way to access this model for reproducing the results or a way to reproduce the model (e.g., with an open-source dataset or instructions for how to construct the dataset).
     (d) We recognize that reproducibility may be tricky in some cases, in which case authors are welcome to describe the particular way they provide for reproducibility. In the case of closed-source models, it may be that access to the model is limited in some way (e.g., to registered users), but it should be possible for other researchers to have some path to reproducing or verifying the results.

5. **Open access to data and code**

   Question: Does the paper provide open access to the data and code, with sufficient instructions to faithfully reproduce the main experimental results, as described in supplemental material?

Answer: [Yes]

Justification: See Supplementary Material.

Guidelines:

- The answer NA means that paper does not include experiments requiring code.
- Please see the NeurIPS code and data submission guidelines (`https://nips.cc/public/guides/CodeSubmissionPolicy`) for more details.
- While we encourage the release of code and data, we understand that this might not be possible, so "No" is an acceptable answer. Papers cannot be rejected simply for not including code, unless this is central to the contribution (e.g., for a new open-source benchmark).
- The instructions should contain the exact command and environment needed to run to reproduce the results. See the NeurIPS code and data submission guidelines (`https://nips.cc/public/guides/CodeSubmissionPolicy`) for more details.
- The authors should provide instructions on data access and preparation, including how to access the raw data, preprocessed data, intermediate data, and generated data, etc.
- The authors should provide scripts to reproduce all experimental results for the new proposed method and baselines. If only a subset of experiments are reproducible, they should state which ones are omitted from the script and why.
- At submission time, to preserve anonymity, the authors should release anonymized versions (if applicable).
- Providing as much information as possible in supplemental material (appended to the paper) is recommended, but including URLs to data and code is permitted.

6. **Experimental setting/details**

   Question: Does the paper specify all the training and test details (e.g., data splits, hyperparameters, how they were chosen, type of optimizer, etc.) necessary to understand the results?

   Answer: [Yes]

   Justification: See Subsection 4.1.

   Guidelines:

   - The answer NA means that the paper does not include experiments.
   - The experimental setting should be presented in the core of the paper to a level of detail that is necessary to appreciate the results and make sense of them.
   - The full details can be provided either with the code, in appendix, or as supplemental material.

7. **Experiment statistical significance**

   Question: Does the paper report error bars suitably and correctly defined or other appropriate information about the statistical significance of the experiments?

   Answer: [NA]

   Justification: The paper does not include such experiments.

   Guidelines:

   - The answer NA means that the paper does not include experiments.
   - The authors should answer "Yes" if the results are accompanied by error bars, confidence intervals, or statistical significance tests, at least for the experiments that support the main claims of the paper.
   - The factors of variability that the error bars are capturing should be clearly stated (for example, train/test split, initialization, random drawing of some parameter, or overall run with given experimental conditions).
   - The method for calculating the error bars should be explained (closed form formula, call to a library function, bootstrap, etc.)
   - The assumptions made should be given (e.g., Normally distributed errors).
   - It should be clear whether the error bar is the standard deviation or the standard error of the mean.

- It is OK to report 1-sigma error bars, but one should state it. The authors should preferably report a 2-sigma error bar than state that they have a 96% CI, if the hypothesis of Normality of errors is not verified.
- For asymmetric distributions, the authors should be careful not to show in tables or figures symmetric error bars that would yield results that are out of range (e.g. negative error rates).
- If error bars are reported in tables or plots, The authors should explain in the text how they were calculated and reference the corresponding figures or tables in the text.

8. **Experiments compute resources**

   Question: For each experiment, does the paper provide sufficient information on the computer resources (type of compute workers, memory, time of execution) needed to reproduce the experiments?

   Answer: [Yes]

   Justification: See Section 4 and Appendix.

   Guidelines:

   - The answer NA means that the paper does not include experiments.
   - The paper should indicate the type of compute workers CPU or GPU, internal cluster, or cloud provider, including relevant memory and storage.
   - The paper should provide the amount of compute required for each of the individual experimental runs as well as estimate the total compute.
   - The paper should disclose whether the full research project required more compute than the experiments reported in the paper (e.g., preliminary or failed experiments that didn't make it into the paper).

9. **Code of ethics**

   Question: Does the research conducted in the paper conform, in every respect, with the NeurIPS Code of Ethics `https://neurips.cc/public/EthicsGuidelines`?

   Answer: [Yes]

   Justification: The research conducted in the paper conforms, in every respect, with the NeurIPS Code of Ethics.

   Guidelines:

   - The answer NA means that the authors have not reviewed the NeurIPS Code of Ethics.
   - If the authors answer No, they should explain the special circumstances that require a deviation from the Code of Ethics.
   - The authors should make sure to preserve anonymity (e.g., if there is a special consideration due to laws or regulations in their jurisdiction).

10. **Broader impacts**

    Question: Does the paper discuss both potential positive societal impacts and negative societal impacts of the work performed?

    Answer: [Yes]

    Justification: See Section A7 in Appendix.

    Guidelines:

    - The answer NA means that there is no societal impact of the work performed.
    - If the authors answer NA or No, they should explain why their work has no societal impact or why the paper does not address societal impact.
    - Examples of negative societal impacts include potential malicious or unintended uses (e.g., disinformation, generating fake profiles, surveillance), fairness considerations (e.g., deployment of technologies that could make decisions that unfairly impact specific groups), privacy considerations, and security considerations.

- The conference expects that many papers will be foundational research and not tied to particular applications, let alone deployments. However, if there is a direct path to any negative applications, the authors should point it out. For example, it is legitimate to point out that an improvement in the quality of generative models could be used to generate deepfakes for disinformation. On the other hand, it is not needed to point out that a generic algorithm for optimizing neural networks could enable people to train models that generate Deepfakes faster.
- The authors should consider possible harms that could arise when the technology is being used as intended and functioning correctly, harms that could arise when the technology is being used as intended but gives incorrect results, and harms following from (intentional or unintentional) misuse of the technology.
- If there are negative societal impacts, the authors could also discuss possible mitigation strategies (e.g., gated release of models, providing defenses in addition to attacks, mechanisms for monitoring misuse, mechanisms to monitor how a system learns from feedback over time, improving the efficiency and accessibility of ML).

11. **Safeguards**

    Question: Does the paper describe safeguards that have been put in place for responsible release of data or models that have a high risk for misuse (e.g., pretrained language models, image generators, or scraped datasets)?

    Answer: [NA]

    Justification: The paper poses no such risks.

    Guidelines:

    - The answer NA means that the paper poses no such risks.
    - Released models that have a high risk for misuse or dual-use should be released with necessary safeguards to allow for controlled use of the model, for example by requiring that users adhere to usage guidelines or restrictions to access the model or implementing safety filters.
    - Datasets that have been scraped from the Internet could pose safety risks. The authors should describe how they avoided releasing unsafe images.
    - We recognize that providing effective safeguards is challenging, and many papers do not require this, but we encourage authors to take this into account and make a best faith effort.

12. **Licenses for existing assets**

    Question: Are the creators or original owners of assets (e.g., code, data, models), used in the paper, properly credited and are the license and terms of use explicitly mentioned and properly respected?

    Answer: [Yes]

    Justification: All the existing assets used are properly cited or credited in the paper.

    Guidelines:

    - The answer NA means that the paper does not use existing assets.
    - The authors should cite the original paper that produced the code package or dataset.
    - The authors should state which version of the asset is used and, if possible, include a URL.
    - The name of the license (e.g., CC-BY 4.0) should be included for each asset.
    - For scraped data from a particular source (e.g., website), the copyright and terms of service of that source should be provided.
    - If assets are released, the license, copyright information, and terms of use in the package should be provided. For popular datasets, `paperswithcode.com/datasets` has curated licenses for some datasets. Their licensing guide can help determine the license of a dataset.
    - For existing datasets that are re-packaged, both the original license and the license of the derived asset (if it has changed) should be provided.

- If this information is not available online, the authors are encouraged to reach out to the asset's creators.

13. **New assets**

    Question: Are new assets introduced in the paper well documented and is the documentation provided alongside the assets?

    Answer: [NA]

    Justification: The paper does not release new assets.

    Guidelines:

    - The answer NA means that the paper does not release new assets.
    - Researchers should communicate the details of the dataset/code/model as part of their submissions via structured templates. This includes details about training, license, limitations, etc.
    - The paper should discuss whether and how consent was obtained from people whose asset is used.
    - At submission time, remember to anonymize your assets (if applicable). You can either create an anonymized URL or include an anonymized zip file.

14. **Crowdsourcing and research with human subjects**

    Question: For crowdsourcing experiments and research with human subjects, does the paper include the full text of instructions given to participants and screenshots, if applicable, as well as details about compensation (if any)?

    Answer: [NA]

    Justification: The paper does not involve crowdsourcing nor research with human subjects.

    Guidelines:

    - The answer NA means that the paper does not involve crowdsourcing nor research with human subjects.
    - Including this information in the supplemental material is fine, but if the main contribution of the paper involves human subjects, then as much detail as possible should be included in the main paper.
    - According to the NeurIPS Code of Ethics, workers involved in data collection, curation, or other labor should be paid at least the minimum wage in the country of the data collector.

15. **Institutional review board (IRB) approvals or equivalent for research with human subjects**

    Question: Does the paper describe potential risks incurred by study participants, whether such risks were disclosed to the subjects, and whether Institutional Review Board (IRB) approvals (or an equivalent approval/review based on the requirements of your country or institution) were obtained?

    Answer: [NA]

    Justification: The paper does not involve crowdsourcing nor research with human subjects.

    Guidelines:

    - The answer NA means that the paper does not involve crowdsourcing nor research with human subjects.
    - Depending on the country in which research is conducted, IRB approval (or equivalent) may be required for any human subjects research. If you obtained IRB approval, you should clearly state this in the paper.
    - We recognize that the procedures for this may vary significantly between institutions and locations, and we expect authors to adhere to the NeurIPS Code of Ethics and the guidelines for their institution.
    - For initial submissions, do not include any information that would break anonymity (if applicable), such as the institution conducting the review.

16. **Declaration of LLM usage**

Question: Does the paper describe the usage of LLMs if it is an important, original, or non-standard component of the core methods in this research? Note that if the LLM is used only for writing, editing, or formatting purposes and does not impact the core methodology, scientific rigorousness, or originality of the research, declaration is not required.

Answer: [NA]

Justification: The core method development in this research does not involve LLMs as any important, original, or non-standard components.

Guidelines:

- The answer NA means that the core method development in this research does not involve LLMs as any important, original, or non-standard components.
- Please refer to our LLM policy (`https://neurips.cc/Conferences/2025/LLM`) for what should or should not be described.

A1 Upper bounds analysis

The following derivations omit the normalization term of the softmax operation for convenience. To characterize the difference between $\boldsymbol{H}$ and $\boldsymbol{H}_1$, we set $\mathbb{I}_i = \{(i-1)b+1, (i-1)b+2, \ldots, ib\}$ with $i = 1, 2, \ldots, m/b$. Then the entries of $\boldsymbol{A}_1$ can also be defined as $\boldsymbol{A}_1(\mathbb{I}_i, \mathbb{I}_i) = \boldsymbol{A}(\mathbb{I}_i, \mathbb{I}_i)$ with $i = 1, 2, \ldots, m/b$, and $\boldsymbol{A}_1(\mathbb{I}_i, \mathbb{I}_{i'}) = \boldsymbol{0}_b$ with $i \neq i'$, where $\boldsymbol{0}_b \in \mathbb{R}^{b\times b}$ is the all-zeros matrix. Hence, we have

$$\|\boldsymbol{A}_1 - \boldsymbol{A}\|_F \leq \sum_{i,i'=1, i\neq i'}^{m/b} \|\boldsymbol{A}(\mathbb{I}_i, \mathbb{I}_{i'})\|_F,$$

which implies that

$$\|\boldsymbol{H}_1 - \boldsymbol{H}\|_F = \|\boldsymbol{A}_1\boldsymbol{V} - \boldsymbol{A}\boldsymbol{V}\|_F \leq \sum_{i,i'=1, i\neq i'}^{m/b} \|\boldsymbol{A}(\mathbb{I}_i, \mathbb{I}_{i'})\|_F \|\boldsymbol{V}\|_F. \tag{A1}$$

For $\|\boldsymbol{A}' - \boldsymbol{A}\|_F$ and $\|\boldsymbol{A}'' - \boldsymbol{A}\|_F$, according to Remarks 1 and 2 we have

$$\|\boldsymbol{A}' - \boldsymbol{A}\|_F \leq \sum_{j,j'=1, j\neq j'}^{b} \|\boldsymbol{A}(\mathbb{J}_j, \mathbb{J}_{j'})\|_F; \tag{A2}$$

$$\begin{aligned}\|\boldsymbol{A}'' - \boldsymbol{A}\|_F &\leq \sum_{k=2}^{b} \|\boldsymbol{A}''_k\|_F + \sum_{j,j'=1, j\neq j'}^{b} \|\boldsymbol{A}(\mathbb{J}_j, \mathbb{J}_{j'})\|_F \\ &\leq \sum_{k=2}^{b}\sum_{j=1}^{b} \|\boldsymbol{A}(\mathbb{J}_j^{(k)}, \mathbb{J}_j^{(k)})\|_F + \sum_{j,j'=1, j\neq j'}^{b} \|\boldsymbol{A}(\mathbb{J}_j^{(1)}, \mathbb{J}_{j'}^{(1)})\|_F.\end{aligned} \tag{A3}$$

Remark 3. Based on the above descriptions and Eqs. (6) and (7), the upper bound for $\|\boldsymbol{H}_2 - \boldsymbol{H}\|_F$ can be discussed in following two cases.

Case (6) corresponding to Eq. (6): an upper bound for $\|\boldsymbol{H}_2 - \boldsymbol{H}\|_F$ is deduced as

$$\begin{aligned}&\|\boldsymbol{H}_2 - \boldsymbol{H}\|_F = \|\boldsymbol{A}''\boldsymbol{A}_1\boldsymbol{V} - \boldsymbol{A}\boldsymbol{V}\|_F = \|\boldsymbol{A}''\boldsymbol{A}_1\boldsymbol{V} - \boldsymbol{A}_1\boldsymbol{V} + \boldsymbol{A}_1\boldsymbol{V} - \boldsymbol{A}\boldsymbol{V}\|_F \\ &\leq \|\boldsymbol{A}''\boldsymbol{A}_1\boldsymbol{V} - \boldsymbol{A}_1\boldsymbol{V}\|_F + \|\boldsymbol{A}_1\boldsymbol{V} - \boldsymbol{A}\boldsymbol{V}\|_F \\ &\leq \|\boldsymbol{A}'' - \boldsymbol{I}_m\|_{\max}\|\boldsymbol{A}_1\boldsymbol{V}\|_F + \sum_{i,i'=1, i\neq i'}^{m/b} \|\boldsymbol{A}(\mathbb{I}_i, \mathbb{I}_{i'})\|_F \|\boldsymbol{V}\|_F \\ &\leq \|\boldsymbol{A}'' - \boldsymbol{I}_m\|_{\max}\|\boldsymbol{A}\boldsymbol{V}\|_F + (\|\boldsymbol{A}'' - \boldsymbol{I}_m\|_{\max} + 1) \sum_{i,i'=1, i\neq i'}^{m/b} \|\boldsymbol{A}(\mathbb{I}_i, \mathbb{I}_{i'})\|_F \|\boldsymbol{V}\|_F;\end{aligned} \tag{A4}$$

Case (7) corresponding to Eq. (7): similar to Case (6), an upper bound for $\|\boldsymbol{H}_2 - \boldsymbol{H}\|_F$ is given as

$$\begin{aligned}\|\boldsymbol{H}_2 - \boldsymbol{H}\|_F \leq &\|\boldsymbol{A}' - \boldsymbol{I}_m\|_{\max}\|\boldsymbol{A}\boldsymbol{V}\|_F \\ &+ (\|\boldsymbol{A}' - \boldsymbol{I}_m\|_{\max} + 1) \sum_{i,i'=1, i\neq i'}^{m/b} \|\boldsymbol{A}(\mathbb{I}_i, \mathbb{I}_{i'})\|_F \|\boldsymbol{V}\|_F,\end{aligned} \tag{A5}$$

where for any matrix $\boldsymbol{B} \in \mathbb{R}^{m\times n}$, the symbol $\|\boldsymbol{B}\|_{\max}$ is defined as

$$\|\boldsymbol{B}\|_{\max} = \max\{|b_{ij}| : i = 1, 2, \ldots, m; j = 1, 2, \ldots, n\}.$$

We now estimate two terms $\|\boldsymbol{A}'' - \boldsymbol{I}_m\|_{\max}$ and $\|\boldsymbol{A}' - \boldsymbol{I}_m\|_{\max}$ in Remark 3 based on Inequalities (A2) and (A3) as follows:

$$\begin{aligned}&\|\boldsymbol{A}'' - \boldsymbol{I}_m\|_{\max} = \|\boldsymbol{A}'' - \boldsymbol{A} + \boldsymbol{A} - \boldsymbol{I}_m\|_{\max} \leq \|\boldsymbol{A}'' - \boldsymbol{A}\|_{\max} + \|\boldsymbol{A} - \boldsymbol{I}_m\|_{\max} \leq \|\boldsymbol{A}'' - \boldsymbol{A}\|_F \\ &+ \|\boldsymbol{A} - \boldsymbol{I}_m\|_{\max} \leq \sum_{k=2}^{b}\sum_{j=1}^{b} \|\boldsymbol{A}(\mathbb{J}_j^{(k)}, \mathbb{J}_j^{(k)})\|_F + \sum_{j,j'=1, j\neq j'}^{b} \|\boldsymbol{A}(\mathbb{J}_j^{(1)}, \mathbb{J}_{j'}^{(1)})\|_F + \|\boldsymbol{A} - \boldsymbol{I}_m\|_{\max},\end{aligned} \tag{A6}$$

and

$$\|\boldsymbol{A}' - \boldsymbol{I}_m\|_{\max} \leq \sum_{j,j'=1,j\neq j'}^{b} \|\boldsymbol{A}(\mathbb{J}_j, \mathbb{J}_{j'})\|_F + \|\boldsymbol{A} - \boldsymbol{I}_m\|_{\max}. \tag{A7}$$

Therefore, the upper bound for $\|\boldsymbol{H}_2 - \boldsymbol{H}\|_F$ in Case (6) is obtained by combining Inequalities (A4) and (A6):

$$\|\boldsymbol{H}_2 - \boldsymbol{H}\|_F \leq \alpha \|\boldsymbol{A}\boldsymbol{V}\|_F + \beta \sum_{i,i'=1,i\neq i'}^{m/b} \|\boldsymbol{A}(\mathbb{I}_i, \mathbb{I}_{i'})\|_F \|\boldsymbol{V}\|_F \tag{A8}$$

with

$$\alpha = \sum_{k=2}^{b}\sum_{j=1}^{b} \|\boldsymbol{A}(\mathbb{J}_j^{(k)}, \mathbb{J}_j^{(k)})\|_F + \sum_{j,j'=1,j\neq j'}^{b} \|\boldsymbol{A}(\mathbb{J}_j^{(1)}, \mathbb{J}_{j'}^{(1)})\|_F + \|\boldsymbol{A} - \boldsymbol{I}_m\|_{\max}, \quad \beta = \alpha + 1,$$

and the upper bound for $\|\boldsymbol{H}_2 - \boldsymbol{H}\|_F$ in Case (7) is obtained by combining Inequalities (A5) and (A7):

$$\|\boldsymbol{H}_2 - \boldsymbol{H}\|_F \leq \alpha' \|\boldsymbol{A}\boldsymbol{V}\|_F + \beta' \sum_{i,i'=1,i\neq i'}^{m/b} \|\boldsymbol{A}(\mathbb{I}_i, \mathbb{I}_{i'})\|_F \|\boldsymbol{V}\|_F \tag{A9}$$

with

$$\alpha' = \sum_{j,j'=1,j\neq j'}^{b} \|\boldsymbol{A}(\mathbb{J}_j, \mathbb{J}_{j'})\|_F + \|\boldsymbol{A} - \boldsymbol{I}_m\|_{\max}, \quad \beta' = \alpha' + 1.$$

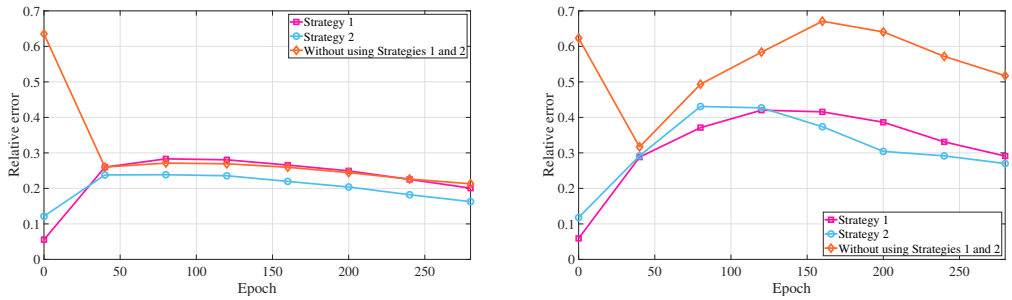

(a) Backbone: CSWin-T (b) Backbone: Swin-T

Figure A1: The comparison of relative error of DuSA using Strategy 1 (its relative approximation error is: $\frac{\|\boldsymbol{H}_2 - \boldsymbol{H}\|_F}{\|\boldsymbol{H}\|_F}$ and the upper bound of the term $\|\boldsymbol{H}_2 - \boldsymbol{H}\|_F$ can be obtained using Inequality (A9)), DuSA using Strategy 2 (its relative approximation error is: $\frac{\|\boldsymbol{H}_2 - \boldsymbol{H}\|_F}{\|\boldsymbol{H}\|_F}$ and the upper bound of the term $\|\boldsymbol{H}_2 - \boldsymbol{H}\|_F$ can be obtained using Inequality (A8)), and DuSA without using Strategies 1 and 2 (its relative approximation error is: $\frac{\|\boldsymbol{H}_1 - \boldsymbol{H}\|_F}{\|\boldsymbol{H}\|_F}$ and the upper bound of the term $\|\boldsymbol{H}_1 - \boldsymbol{H}\|_F$ can be obtained using Inequality (A1)) in approximating VSA during the training of CSWin-T/Swin-T on ImageNet-1K. The approximation error shows a decreasing trend. Strategy 1 shows a lower error curve at the beginning of training which is consistent with the analysis of the relationship between the upper bound Inequality (A8) and the upper bound Inequality (A9). As the training process progresses, the actual approximation error of Strategy 2 becomes even smaller than the actual approximation error of Strategy 1 which is also consistent with more token information introduced by Strategy 2 in token mixing to enhance performance. Even the backbone is untrained, DuSA using Strategy 1 or 2 still provides significantly lower approximation error than DuSA without using Strategies 1 and 2 which further demonstrates that DuSA is more similar to VSA than simple sliding window based sparse attention.

Remark 4. For the term $\|\boldsymbol{H}_2 - \boldsymbol{H}\|_F$, its upper bound (A8) or (A9) may be relatively rough. In the future, a key issue is to obtain a tighter upper bound for $\|\boldsymbol{H}_2 - \boldsymbol{H}\|_F$ in Cases (6) and (7). Fig. A1 shows the comparison of the actual relative error of DuSA using blockify Strategy 1, DuSA using blockify Strategy 2, and DuSA without using blockify Strategies 1 and 2 in approximating VSA. Blockify Strategy 1 shows a lower error curve at the beginning of training which is consistent with the analysis of the relationship between the upper bound Inequality (A8) and the upper bound Inequality (A9). As the training process progresses, the actual approximation error of blockify Strategy 2 becomes even smaller than the actual approximation error of blockify Strategy 1 which is also consistent with more token information introduced by blockify Strategy 2 in token mixing to enhance performance. Even the backbone is untrained, DuSA using blockify Strategy 1 or 2 still provides significantly lower approximation error than DuSA without using blockify Strategies 1 and 2 which further demonstrates that DuSA is more similar to VSA than simple sliding window based sparse attention (DuSA without using blockify Strategies 1 and 2).

Table A1: ImageNet-1K classification comparison. Note: FPS was measured on 1 NVIDIA H20 using a batch size of 512 for tiny models and 256/32 for base models with a resolution of 224^2/384^2 and mixed precision.

Method	Resolution	Accuracy (%)	FPS (imgs/s)	#	FLOPs
			CSWin-B		
Agent	224^2 | 384^2	84.7 | 85.8	994 | 276	73M	14.49G | 42.57G
EFFATT	224^2 | 384^2	84.4 | 85.7	1059 | 331	73M	14.53G | 42.69G
ELFATT	224^2 | 384^2	84.7 | 85.8	1187 | 355	73M	14.46G | 42.48G
FLatten	224^2 | 384^2	84.5 | 85.5	864 | 266	75M	14.52G | 42.67G
LOCAL	224^2 | 384^2	84.4 | 85.5	1037 | 323	73M	14.39G | 42.28G
VSA	224^2 | 384^2	84.7 | 85.9	478/879 (FA2) | 82/201 (FA2)	73M	22.33G/14.39G (FA2) | 110.89G/42.28G (FA2)
DuSA	224^2 | 384^2	84.7 | 85.9	1203 | 356	73M	14.39G | 42.28G
			CSWin-T		
Agent	224^2	83.1	2425	20M	4.14G
EFFATT	224^2	82.6	2526	20M	4.17G
ELFATT	224^2	83.1	2856	20M	4.13G
FLatten	224^2	83.1	2025	21M	4.16G
LOCAL	224^2	82.7	2519	20M	4.09G
VSA	224^2	83.1	1303/2210 (FA2)	20M	7.60G/4.09G (FA2)
DuSA	224^2	83.2	2908	20M	4.09G
			Swin-B		
Agent	224^2 | 384^2	84.0 | 84.9	1367 | 372	88M	15.44G | 46.34G
EFFATT	224^2 | 384^2	84.2 | 85.3	1536 | 481	88M	15.33G | 45.04G
ELFATT	224^2 | 384^2	84.5 | 85.5	1497 | 457	91M	15.68G | 46.08G
FLatten	224^2 | 384^2	83.8 | 85.0	1226 | 353	89M	15.46G | 46.49G
LOCAL	224^2 | 384^2	83.5 | 84.5	1351 | 357	88M	15.47G | 47.19G
VSA	224^2 | 384^2	84.2 | 85.3	743/1325 (FA2) | 134/313 (FA2)	88M	21.57G/15.19G (FA2) | 99.76G/44.64G (FA2)
DuSA	224^2 | 384^2	84.5 | 85.5	1568 | 485	91M	15.61G | 45.88G
			Swin-T		
Agent	224^2	82.6	2847	29M	4.53G
EFFATT	224^2	82.1	3282	28M	4.45G
ELFATT	224^2	82.7	3159	30M	4.67G
FLatten	224^2	82.1	2502	29M	4.50G
LOCAL	224^2	81.4	2943	28M	4.51G
VSA	224^2	82.4	1269/2571 (FA2)	28M	8.81G/4.38G (FA2)
DuSA	224^2	82.7	3154	30M	4.63G
			Others		
ConvNeXt-T	224^2	82.1	3911	29M	4.47G
VMamba-T	224^2	82.5	1837	30M	4.84G

A2 Complexity analysis

For VSA, the nature of the scaled-dot product attention calculation leads to the complexity of $O(m^2 \times c)$. For blockify Strategy 1, the complexity of DuSA is determined by Eqs. (3) and (4). In Eq. (3), the complexity of the computation of the attention matrix $\boldsymbol{A}_1$ is $O(m \times b \times c)$ and the complexity of the token mixing to obtain $\boldsymbol{H}'$ is also $O(m \times b \times c)$. Hence, the total complexity of Eq. (3) is $O(m \times b \times c)$. Similarly, for the complexity of Eq. (4), its complexity is $O((m^2/b) \times c)$. The total complexity of DuSA using blockify Strategy 1 is $O(\frac{m \times b^2 + m^2}{b} \times c)$, and it can achieve the

minimum $O(m \times \sqrt{m} \times c)$ when $b = \sqrt{m}$. For blockify Strategy 2, compared to blockify Strategy 1, it only has one more attention score aggregation process, as shown in Eq. (5) of which the complexity is $O(m^2/b) \ll O((m^2/b) \times c)$. Hence, the total complexity of DuSA using blockify Strategy 2 is also $O(\frac{m \times b^2 + m^2}{b} \times c)$ and its minimum is also $O(m \times \sqrt{m} \times c)$ when $b = \sqrt{m}$. If $m \gg c$, the complexity of DuSA is $O(m \times \sqrt{m})$, which is less than $O(m^2)$ of VSA. Our method is designed for acceleration when $m \gg c$. The larger m is than c, the more obvious the acceleration effect is.

Table A2: The effect of different block sizes at each level (L1-L4) on the performance of DuSA and some plug and play (PP) examples using DuSA to replace VSA directly without training in the ImageNet-1K classification task. Note: FPS was measured on 1 NVIDIA H20 using a batch size of 512 and mixed precision. "PT" denotes the models pre-trained from scratch. CSWin-T-VSA here is the same as CSWin-T-VSA in Table A1 while Swin-T-VSA here uses the enhanced version from [18] which replaces the concatenation operations for partition/merging with convolutions to enhance performance, hence it is a little different from Swin-T-VSA in Table A1.

Block size of each level				Resolution	Accuracy (PT/PP)	FPS (imgs/s)	#	FLOPs
L1	L2	L3	L4					
CSWin-T								
49	49	196	49	224^2	82.7/78.8	2989	20M	4.09G
196	196	196	49	224^2	83.2/82.0	2908	20M	4.09G
784	784	196	49	224^2	83.2/83.1	2860	20M	4.09G
VSA (full sequence length)				224^2	83.1/ —	1303/2210 (FA2)	20M	7.60G/4.09G (FA2)
3136	784	196	49					
Swin-T								
49	49	196	49	224^2	82.5/73.1	3223	30M	4.63G
196	196	196	49	224^2	82.7/80.3	3154	30M	4.63G
784	784	196	49	224^2	82.8/82.4	2958	30M	4.63G
VSA (full sequence length)				224^2	82.7/ —	1188/2257 (FA2)	30M	9.06G/4.63G (FA2)
3136	784	196	49					

A3 The effect of different block sizes and plug and play examples

Table A2 shows the effect of different block sizes at each level (L1-L4) on the performance of DuSA and some plug and play (PP) examples using DuSA to replace VSA directly without training in the ImageNet-1K classification task. The sequence lengths of VSA in 4 levels of CSWin-T/Swin-T are $[3136, 784, 196, 49]$. The sequence lengths of the last two levels are too short to affect ViT speed [7, 16–18]. Hence, we only modified the block sizes of the first two levels. As the block sizes increase, the inference speed is reduced and the accuracy is improved. Even using the 75% sparsity ratio of the first level, DuSA still offers a 1.3× speedup over FA2 in Table A2 and outperforms VSA. Also, as Table A2 shows, when using the 75%-94% sparsity ratios of the first two levels, DuSA can almost maintain 97%+ accuracy in a plug and play application. The current version of DuSA is a static sparse attention mechanism, which cannot preserve the accuracy of VSA without loss in a plug and play application. It is designed for accelerating both the training and inference processes. After training, it can match or even outperform VSA. Inspired by XAttention, we have provided a training-free dynamic sparse attention version of DuSA for accelerating the prefilling stage of large language models (LLMs). The dynamic version of DuSA can match the performance of VSA in plug and play applications and provides a significant acceleration effect. Details are available in Section A6.

A4 The use of DuSA in simple and general architectures

Table A3 shows the performance comparison of vanilla ViT architectures and the versions using DuSA to replace VSA. The sequence length m of the vanilla ViT architecture is relatively short (for the input resolution of 224^2/384^2 using a constant input patch size of 16, $m = 197/577$ with a constant embedding dimension $c = 64$), which limits the acceleration effect of DuSA and cannot completely show the superiority of DuSA for acceleration. Because DuSA is designed for acceleration when $m \gg c$.

Table A3: The performance comparison of vanilla ViT architectures and the versions using DuSA to replace VSA. All models are trained from scratch on ImageNet-1K. Block size b is 14/24 for tiny(T)/large(L) models. Padding is used to make the sequence length divisible by b. FPS and the inference memory are obtained on 1 NVIDIA H20 using a batch size of 512/32 for the T/L models.

Method	Resolution	Accuracy (%)	FPS (imgs/s)	#	FLOPs	Inference memory (GB)
ViT-L/16-VSA	384^2	76.5	179/272 (FA2)	307M	191.21G/174.85G (FA2)	3.7/**2.9** (FA2)
ViT-L/16-DuSA	384^2	**77.2**	230	307M	174.54G	3.0
ViT-T/16-VSA	224^2	72.6	10644/15350 (FA2)	6M	1.26G/1.08G (FA2)	2.2/**2.0** (FA2)
ViT-T/16-DuSA	224^2	**72.9**	10718	6M	1.07G	**2.0**

A5 Memory consumption patterns of DuSA

Tables A4 and A5 show the memory comparison results. Compared to ELFATT and FA2, DuSA still has the overall lowest memory usage and its memory usage is significantly lower than that of VSA.

Table A4: Peak memory usage comparison on ImageNet-1K using 1 NVIDIA H20 (96GB). The batch size used is 32 in both inference and training. "OOM" denotes out of memory (MEM).

Method	Resolution	Inference MEM (GB)	Training MEM (GB)
CSWin-B-ELFATT	384^2	2.5	18.8
CSWin-B-VSA	384^2	62.3/2.4 (FA2)	OOM/**17.9** (FA2)
CSWin-B-DuSA	384^2	**2.3**	21.0

Table A5: Peak memory usage comparison on ADE20K and MS COCO 2017 using 1 NVIDIA H20 (96GB). The batch size used is 1 for inference and 2 for training. "OOM" denotes out of memory.

Method	ADE20K inference MEM (GB)	COCO inference MEM (GB)	ADE20K training MEM (GB)	COCO training MEM (GB)
		Swin-T		
ELFATT	2.8	1.6	5.6	8.2
VSA	49.2/2.8 (FA2)	71.9/1.5 (FA2)	20.1/**5.5** (FA2)	OOM/8.4 (FA2)
DuSA	**2.5**	**1.4**	**5.5**	**8.1**
		CSWin-T		
ELFATT	**2.7**	**1.4**	5.5	8.8
VSA	33.2/**2.7** (FA2)	48.2/**1.4** (FA2)	16.7/**5.4** (FA2)	OOM/8.8 (FA2)
DuSA	**2.7**	**1.4**	**5.4**	**8.7**

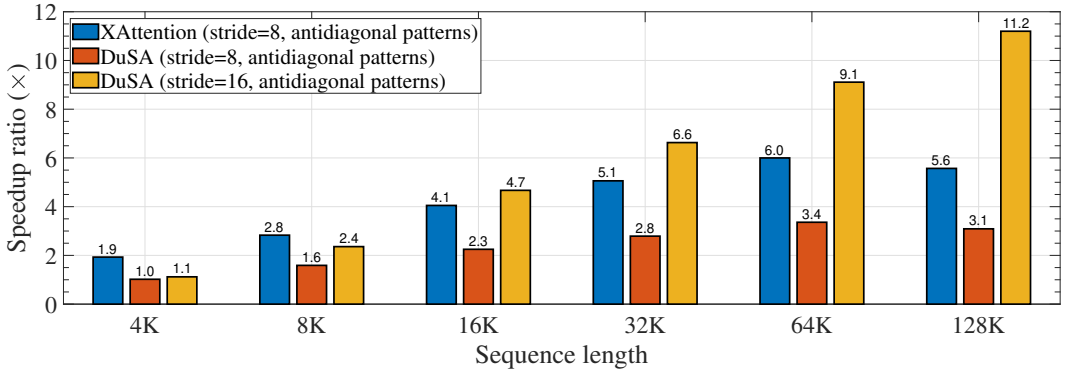

Figure A2: Speedup relative to FlashAttention of FlashInfer obtained by different methods across different sequence lengths using Llama-3.1-8B-Instruct on 1 NVIDIA H20.

A6 The application of DuSA in accelerating the prefilling stage of LLMs

Based on XAttention, we introduce DuSA (Strategy 2: Rolling indices-based attention scores fusion) to search antidiagonal/diagonal patterns of attention matrices to filter important or unimportant blocks for further dynamic sparse attention performed within important blocks only. As Fig. A2 and Table

A6 show, DuSA can use a larger stride (larger sparsity) to achieve similar or higher performance than XAttention, further accelerating FlashAttention of FlashInfer. By introducing antidiagonal patterns of XAttention, the performance of DuSA can be further improved.

Table A6: The performance comparison of different attention methods on LongBench using the Llama-3.1-8B-Instruct model. Note: Higher scores mean better performance.

NarrativeQA	Qasper	MultiFieldQA-en	MultiFieldQA-zh	HotpotQA	2WikiMultihopQA	MuSiQue	DuReader	GovReport	QMSum	MultiNews	VCSUM	TREC	TriviaQA	SAMSum	LSHT	PassageCount	PassageRetrieval-en	PassageRetrieval-zh	LCC	RepoBench-P	Average
VSA (FlashAttention of FlashInfer)																					
31.44	25.07	**29.40**	**61.68**	16.89	17.00	11.79	34.93	34.22	23.25	26.69	15.91	72.50	91.65	43.74	46.00	5.95	**98.20**	**77.11**	52.19	49.14	**41.18**
XAttention (stride=8, antidiagonal patterns)																					
30.48	26.04	29.28	61.67	17.33	16.34	11.88	34.64	34.60	23.24	27.08	16.11	71.50	90.97	**44.13**	46.50	5.23	88.68	74.40	53.23	**50.94**	40.68
DuSA (stride=8, antidiagonal patterns)																					
30.81	24.28	28.88	58.28	**18.09**	16.03	10.21	35.40	**34.68**	23.21	26.92	15.77	72.50	**92.15**	43.27	**47.00**	**7.25**	96.84	76.67	52.28	48.97	40.92
DuSA (stride=8, diagonal patterns)																					
31.34	25.96	28.78	61.65	16.92	16.35	11.86	35.60	34.54	**23.43**	**27.17**	**16.21**	**73.00**	90.62	43.59	46.50	6.38	89.26	75.06	53.24	50.16	40.84
DuSA (stride=16, antidiagonal patterns)																					
30.21	**27.57**	29.00	60.99	17.34	**17.02**	**12.04**	**36.13**	34.59	23.18	26.96	15.73	71.50	90.90	43.67	46.00	6.39	97.76	73.76	**53.36**	49.56	41.13

A7 Broader impacts

DuSA provides an efficient attention mechanism to accelerate training and inference of long-context transformers, and it is not hardware-aware, which will benefit academia and startups to reduce deployment costs using medium-performance GPUs and unlock cross-disciplinary breakthroughs. DuSA can be used in advanced hierarchical sparse attention mechanisms to improve their performance and speed as a novel alternative for basic sparse attention. Although the enhanced efficiency of long-context transformers may increase risks such as misuse in generating fake/harmful contents, the benefits brought by efficient long-context transformers outweigh the risks in general.

A8 Limitations

As Remark 4 shows, for the term $\|\boldsymbol{H}_2 - \boldsymbol{H}\|_F$, its upper bound (Inequality (A8) or (A9)) provides a worst-case guarantee and may be relatively rough: In the current version, the upper bound (Inequality (A8) or (A9)) for Strategy 1 or 2 is larger than the upper bound (Inequality (A1)) for simple block sparse attention. However, as shown in Fig. A1, the actual approximation error of DuSA (Strategy 1) or DuSA (Strategy 2) is usually much lower than that of DuSA without using Strategies 1 and 2. In the future, a key issue is to obtain a tighter upper bound for Strategy 1 or 2. In addition, the acceleration effect of DuSA may be limited when m is not significantly larger than c.